

Optimal Relay Selection for the Parallel Hybrid RF/FSO Relay Channel: Non-Buffer-Aided and Buffer-Aided Designs

Marzieh Najafi, Vahid Jamali, and Robert Schober

Friedrich-Alexander University (FAU), Erlangen, Germany

Abstract

Hybrid radio frequency (RF)/free space optical (FSO) systems are among the candidate enabling technologies for the next generation of wireless networks since they benefit from both the high data rates of the FSO subsystem and the high reliability of the RF subsystem. In this paper, we focus on the problem of throughput maximization in the parallel hybrid RF/FSO relay channel. In the parallel hybrid RF/FSO relay channel, a source node sends its data to a destination node with the help of multiple relay nodes. Thereby, for a given relay, the source-relay and the relay-destination FSO links are orthogonal with respect to each other due to the narrow beam employed for FSO transmission, whereas, due to the broadcast nature of the RF channel, half-duplex operation is required for the RF links if self-interference is to be avoided. Moreover, we consider the two cases where the relays are and are not equipped with buffers. For both cases, we derive the optimal relay selection policies for the RF and FSO links and the optimal time allocation policy for transmission and reception for the RF links. The proposed optimal protocols provide important insights for optimal system design. Since the optimal buffer-aided (BA) policy introduces an unbounded end-to-end delay, we also propose a suboptimal BA policy which ensures certain target average delays. Moreover, we present distributed implementations for both proposed optimal protocols. Simulation results demonstrate that a considerable gain can be achieved by the proposed adaptive protocols in comparison with benchmark schemes from the literature.

Index Terms

Adaptive relay selection, hybrid RF/FSO systems, parallel relay channel, buffer-aided relaying, non-buffer-aided relaying, and average delay.

I. INTRODUCTION

The ever-growing demand for higher data rates observed over the last few decades has become the main challenge and research focus for the design of the next generation of wireless communication

systems [1]. In particular, it is expected that by 2020 the number of devices which will use the fifth generation (5G) of wireless communication technology will reach tens or even hundreds of billions [2] and the total required data rate will exceed 500 exabytes [3]. Free space optical (FSO) systems are considered to be a powerful complementary and/or alternative technology to the current radio frequency (RF) systems for meeting the data rate requirements of next generation wireless networks [1]. In addition to the huge usable bandwidth, FSO systems are inherently secure and energy efficient [4].

The aforementioned beneficial properties of FSO systems come at the expense of some drawbacks and challenges which include the requirement of having a line of sight (LOS) between transmitter and receiver, the adverse effects of atmospheric turbulence, and unpredictable connectivity and temporary link outages due to visibility limiting conditions including snow, fog, and dust [4], [5]. Various approaches have been proposed to mitigate these problems. For example, relay-based cooperation has been proposed as an effective strategy to facilitate an LOS between transmitter and receiver [6], [7]. Thereby, the parallel relaying network, where multiple relay nodes assist transmission from a source node to a destination node, is of particular interest [6]–[10]. This network architecture provides spatial diversity which can be exploited to mitigate the fading induced by atmospheric turbulence. Moreover, since RF systems are more reliable in terms of preserving connectivity albeit at lower data rates, hybrid RF/FSO systems, where an additional RF link is employed to support the FSO link, have been proposed. These systems can benefit from both the high data rates of the FSO link and the reliability of the RF link [11], [12].

The parallel FSO relay channel without RF backup links was considered in [6]–[9] and the parallel mixed RF/FSO relay channel with source-relay RF links and relay-destination FSO links was studied in [10]. Furthermore, the mixed RF/FSO relay channel with source-relay RF links and relay-destination hybrid RF/FSO links was considered in [13]. However, to the best of the authors' knowledge, the parallel hybrid RF/FSO relay channel, which is considered in this paper and its conference version [14], has not been investigated in the literature, yet. Such a communication system can be used for example for the wireless backhauling of a small-cell base station (BS) to a macro-cell BS [15] and for forwarding data gathered by a wireless video surveillance camera to a central processing unit [4] via multiple relays. Thereby, the nodes may be located on the roofs of buildings to maintain an LOS as required for FSO. The RF links support the FSO links in case of temporary loss of the LOS due to adverse weather conditions or moving clouds and birds. We consider relay selection since it efficiently exploits the diversity that independent fading realizations offer and entails a significantly lower system complexity compared to transmission schemes where all

relays are active simultaneously [9], [10], [16]. Furthermore, we assume full-duplex transmission for the FSO links owing to the narrow-beam property of FSO, whereas due to the broadcast nature of RF, half-duplex transmission is assumed for the RF links for the sake of simplicity and feasibility¹. For the relays, we consider two cases depending on whether or not they are equipped with buffers. For the non-buffer-aided (non-BA) case, the relay nodes receive data from the source and immediately forward it to the destination. On the other hand, for the buffer-aided (BA) case, the relay nodes can store the data received from the source in their buffers and forward it to the destination when their transmit channel qualities are favorable [18].

For both the non-BA and the BA cases, we derive the optimal relay selection policies for the RF and FSO links such that the end-to-end throughput is maximized. To further improve the throughput, the time allocation between RF transmission and reception for the selected relays is optimized. The proposed protocols provide important insights regarding optimal system design. For instance, the optimal non-BA policy selects at most two different relays for reception and transmission of the RF and FSO signals. In contrast, the optimal BA policy selects at most three different relays. Moreover, we show that depending on which relays are selected for RF and FSO reception/transmission, there are three and ten possible optimal protocol modes for the non-BA and BA policies, respectively. These protocol modes can be further categorized into three types of transmission modes, namely the hybrid mode, the independent mode, and the mixed mode. We show that buffering can considerably enhance the throughput of the considered system at the expense of an increased end-to-end delay [19], [20]. Therefore, we also propose a delay-constrained BA policy which guarantees a certain target average delay. In addition, we develop distribution implementations for the optimal non-BA and BA policies. Our simulation results reveal that a considerable gain can be achieved by the proposed optimal protocols in comparison with benchmark schemes from the literature. Moreover, we show that the proposed delay-constrained BA protocol can approach the performance of the optimal delay-unconstrained BA protocol even for small average delays.

We note that this paper is an extension of our conference paper [14] where only the non-BA case was studied. Moreover, this paper provides distributed implementations for the optimal policies, additional extensive discussions, simulation results, and rigorous proofs which are not included in [14].

The remainder of this paper is organized as follows. In Section II, some preliminaries and assumptions are presented. In Section III, the throughput maximization problems for both the non-

¹Full-duplex RF relays have been reported in the literature [17]. However, they entail high hardware complexity for efficient self-interference suppression. Hence, in this paper, we focus on half-duplex RF relaying.

BA and the BA cases are formulated and the resulting optimal policies are derived. In Section IV, we present solutions to two practical challenges of the proposed optimal policies, namely a delay-constrained BA protocol and distributed implementations for the optimal protocols. Simulation results are provided in Section V and conclusions are drawn in Section VI.

Notations: We use the following notations throughout this paper: $\mathbb{E}\{\cdot\}$ denotes expectation, $|\cdot|$ represents the magnitude of a complex number, $\text{erf}(\cdot)$ is the Gauss-error function, and $\Pr\{A\}$ denotes the probability of the occurrence of event A . Moreover, $\mathbf{0}$ denotes a vector with all elements equal to zero. Additionally, $\text{Rice}(\Omega, \Psi)$ and $\text{GGamma}(\Theta, \Phi)$ denote a Rician random variable (RV) with parameters Ω and Ψ and a Gamma-Gamma RV with parameters Θ and Φ , respectively. For notational convenience, we use the definitions $[x]_a^b \triangleq \min\{b, \max\{a, x\}\}$ for $a \leq b$ and $[x]^+ \triangleq \max\{0, x\}$.

II. PRELIMINARIES AND ASSUMPTIONS

In this section, we present the considered system model, the channel models for the RF and FSO communication links, and the assumptions regarding the required channel state information (CSI).

A. System Model

The system model under consideration is schematically depicted in Fig. 1 a). In particular, source \mathcal{S} wishes to send its information to destination \mathcal{D} via M intermediate relay nodes denoted by \mathcal{R}_m , $m \in \{1, \dots, M\}$. We assume that there is no direct link between \mathcal{S} and \mathcal{D} . Moreover, the $\mathcal{S} - \mathcal{R}_m$ and $\mathcal{R}_m - \mathcal{D}$ links are hybrid RF/FSO where each FSO link is supported by an RF link. Fig. 1 b) shows a possible application scenario of the considered communication system, namely wireless backhauling of a small-cell BS to a macro-cell BS via intermediate relays. The entire time of operation is divided into B equal-length slots satisfying $B \rightarrow \infty$. Moreover, depending on whether or not the relay nodes are equipped with buffers, we consider two different cases namely BA and non-BA relaying. Non-BA relay nodes \mathcal{R}_m have to forward the data received from \mathcal{S} in the *same time slot* to \mathcal{D} . In contrast, BA relays \mathcal{R}_m are allowed to receive data from \mathcal{S} , store it in their buffers, and forward it to \mathcal{D} when the $\mathcal{R}_m - \mathcal{D}$ link quality is favorable.

B. Communication Links

In the following, we describe the adopted channel model for the FSO and RF links.

1) *FSO Links:* We assume that the FSO system employs on-off keying (OOK) with intensity-modulation and direct-detection (IM/DD). Here, \mathcal{S} is equipped with a multi-aperture transmitter pointing in the directions of the relays. Each relay has an aperture directed towards \mathcal{D} and a photodetector for detection of the optical signal received from \mathcal{S} . Furthermore, \mathcal{D} is equipped with

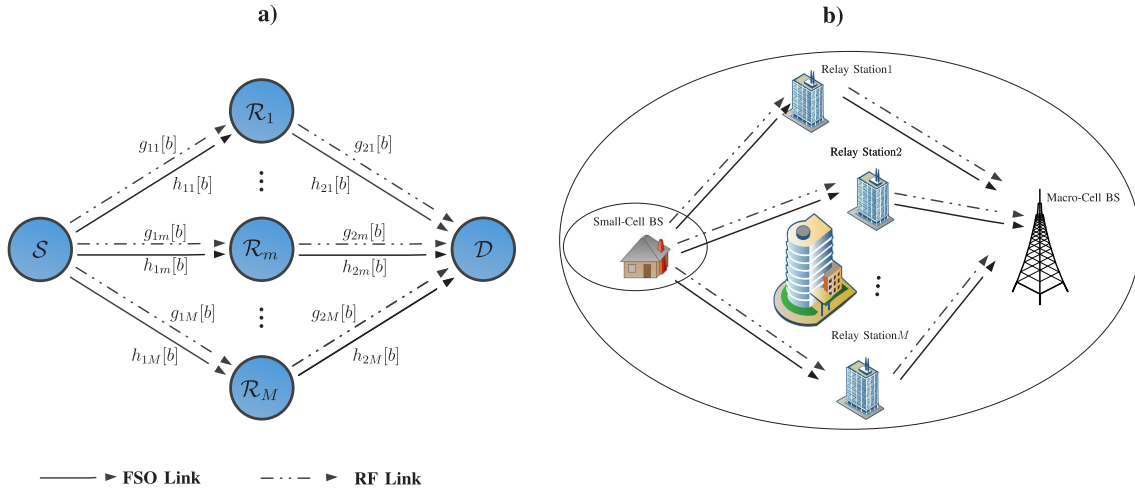


Fig. 1. Parallel hybrid RF/FSO relay channel: a) schematic presentation and b) application scenario for wireless backhauling.

a photodetector for detection of the optical signals received from the relays. Let $y_{1m}^{\text{fso}}[b]$ and $y_{2m}^{\text{fso}}[b]$ denote the intensities of the optical signals received at \mathcal{R}_m and \mathcal{D} in the b -th time slot, respectively. Thereby, after removing the ambient background light intensity, $y_{lm}^{\text{fso}}[b]$ can be modelled as [4], [5]

$$y_{lm}^{\text{fso}}[b] = h_{lm}[b]x_{lm}^{\text{fso}}[b] + z_{lm}^{\text{fso}}[b], \quad l = 1, 2, \quad (1)$$

where $x_{1m}^{\text{fso}}[b] \in \{0, P_S^{\text{fso}}\}$ and $x_{2m}^{\text{fso}}[b] \in \{0, P_{\mathcal{R}_m}^{\text{fso}}\}$ denote the intensities of the optical signals transmitted by \mathcal{S} and \mathcal{R}_m in the b -th time slot, respectively. The maximum intensities of the FSO signals, i.e., P_S^{fso} and $P_{\mathcal{R}_m}^{\text{fso}}$, are mainly limited by restrictions imposed by eye safety regulations [4]. Moreover, $z_{1m}^{\text{fso}}[b]$ and $z_{2m}^{\text{fso}}[b]$ are the intensities of the shot noises caused by ambient light at \mathcal{R}_m and \mathcal{D} in the b -th time slot, respectively. Noises $z_{1m}^{\text{fso}}[b]$ and $z_{2m}^{\text{fso}}[b]$ are modelled as zero-mean real-valued additive white Gaussian noises (AWGNs) with variances σ_{1m}^2 and σ_{2m}^2 , respectively, and are independent from each other and from the transmitted FSO signals. Furthermore, $h_{1m}[b]$ and $h_{2m}[b]$ denote the channel gains of the $\mathcal{S} - \mathcal{R}_m$ and $\mathcal{R}_m - \mathcal{D}$ FSO links in the b -th time slot, respectively, and are modelled as mutually independent, ergodic, and stationary random processes with continuous probability density functions (pdfs). We adopt the widely-accepted Gamma-Gamma turbulence model [4], [12], [21]. Hence, $h_{lm}[b]$, $l = 1, 2$, is modelled as $h_{lm}[b] = \bar{h}_{lm}\tilde{h}_{lm}[b]$, where \bar{h}_{lm} and $\tilde{h}_{lm}[b]$ are the average gain and the fading gain of the FSO links, respectively, and are given by [4], [12], [21]

$$\begin{cases} \bar{h}_{lm} = R \left[\text{erf} \left(\frac{\sqrt{\pi}r}{\sqrt{2}\phi d_{lm}} \right) \right]^2 \times 10^{-k_{lm}d_{lm}/10} \\ \tilde{h}_{lm}[b] \sim \text{GGamma}(\Theta, \Phi), \end{cases} \quad (2)$$

where R denotes the responsivity of the photodetector, r is the aperture radius, ϕ is the divergence angle of the beam, d_{1m} and d_{2m} are the distances between the transmitters and the receivers of the $\mathcal{S} - \mathcal{R}_m$ and $\mathcal{R}_m - \mathcal{D}$ links, respectively, and k_{1m} and k_{2m} are the weather-dependent attenuation factors of the $\mathcal{S} - \mathcal{R}_m$ and $\mathcal{R}_m - \mathcal{D}$ FSO links, respectively. Parameters Θ and Φ of the Gamma-Gamma distribution depend on physical parameters such as the wavelength λ^{fso} and the weather-dependent index of refraction structure parameter C_n^2 , cf. [12, Eqs. (3) and (4)].

From an information theoretical point of view, the considered FSO links can be modelled as binary input-continuous output AWGN channels where the maximum information rate is achieved by uniformly distributed binary inputs [22]. In the b -th time slot, the capacities of the $\mathcal{S} - \mathcal{R}_m$ and $\mathcal{R}_m - \mathcal{D}$ FSO links, denoted by $C_{1m}^{\text{fso}}[b]$ and $C_{2m}^{\text{fso}}[b]$, respectively, for OOK inputs are given by [22]

$$C_{lm}^{\text{fso}}[b] = W^{\text{fso}} \left[1 - \frac{1}{\sqrt{2\pi}} \int_{-\infty}^{\infty} \exp(-t^2) \log_2 \left\{ 1 + \exp \left(-\frac{p_{lm}^2[b]}{2\sigma_{lm}^2} \right) \right. \right. \\ \left. \left. \left[\exp \left(\frac{2tp_{lm}[b]}{\sqrt{2\sigma_{lm}^2}} \right) + \exp \left(-\frac{2tp_{lm}[b]}{\sqrt{2\sigma_{lm}^2}} \right) + \exp \left(-\frac{p_{lm}^2[b]}{2\sigma_{lm}^2} \right) \right] \right\} dt \right], \quad (3)$$

where $p_{1m}[b] = P_S^{\text{fso}} h_{1m}[b]$, $p_{2m}[b] = P_{\mathcal{R}_m}^{\text{fso}} h_{2m}[b]$, and W^{fso} is the bandwidth of the FSO signal.

2) *RF Links*: We consider a standard AWGN channel for the RF links. Moreover, we assume that all RF transmitters and receivers are equipped with a single antenna. Let $y_{1m}^{\text{rf}}[b]$ and $y_{2m}^{\text{rf}}[b]$ denote the RF signals received at \mathcal{R}_m and \mathcal{D} in the b -th time slot, respectively, and be modelled as [23]

$$y_{lm}^{\text{rf}}[b] = g_{lm}[b] x_{lm}^{\text{rf}}[b] + z_{lm}^{\text{rf}}[b], \quad l = 1, 2, \quad (4)$$

where $x_{1m}^{\text{rf}}[b]$ and $x_{2m}^{\text{rf}}[b]$ are the RF signals transmitted by \mathcal{S} and \mathcal{R}_m , respectively. Additionally, $z_{1m}^{\text{rf}}[b]$ and $z_{2m}^{\text{rf}}[b]$ denote the receiver noises at \mathcal{R}_m and \mathcal{D} in the b -th time slot, respectively. We assume that $z_{1m}^{\text{rf}}[b]$ and $z_{2m}^{\text{rf}}[b]$ can be modelled as zero-mean complex AWGNs with variances δ_{1m}^2 and δ_{2m}^2 , respectively. The RF noise variances are given by $[\delta_{lm}^2]_{\text{dB}} = W^{\text{rf}} N_{lm,0} + N_{lm,F}$, where W^{rf} is the bandwidth of the RF signal, $N_{lm,0}$ denotes the noise power spectral density (in dB/Hz), and $N_{lm,F}$ is the noise figure (in dB) of the RF receivers. Furthermore, $g_{1m}[b]$ and $g_{2m}[b]$ are mutually independent, ergodic, and stationary random processes with continuous pdfs specifying the channel coefficients of the $\mathcal{S} - \mathcal{R}_m$ and $\mathcal{R}_m - \mathcal{D}$ RF links in the b -th time slot, respectively. For the hybrid RF/FSO link, an LOS has to be available for the applicability of the FSO system [12], [21]. Therefore, we assume Rician fading for the RF links which includes the effects of both scattered and LOS paths. Taking into account the effect of path-loss, $g_{lm}[b]$ is modelled as $g_{lm}[b] = \sqrt{\bar{g}_{lm}} \tilde{g}_{lm}[b]$, where \bar{g}_{lm} and $\tilde{g}_{lm}[b]$ denote the average gain and the fading coefficient of the RF links, respectively, and

are given by [12], [24]

$$\begin{cases} \bar{g}_{lm} = \left[\frac{\lambda^{\text{rf}} \sqrt{G_{\text{tx}}^{\text{rf}} G_{\text{rx}}^{\text{rf}}}}{4\pi d_{\text{ref}}^{\text{rf}}} \right]^2 \times \left[\frac{d_{\text{ref}}^{\text{rf}}}{d_{lm}} \right]^{\nu_{lm}} \\ |\tilde{g}_{lm}[b]| \sim \text{Rice}(\Omega, \Psi), \end{cases} \quad (5)$$

where λ^{rf} is the wavelength of the RF signal, $G_{\text{tx}}^{\text{rf}}$ and $G_{\text{rx}}^{\text{rf}}$ are the transmit and receive RF antenna gains, respectively, and $d_{\text{ref}}^{\text{rf}}$ denotes a reference distance for the antenna far-field. Moreover, ν_{1m} and ν_{2m} are the path-loss exponents of the $\mathcal{S} - \mathcal{R}_m$ and $\mathcal{R}_m - \mathcal{D}$ RF links, respectively. Parameters Ω and Ψ of the Rice distribution denote the ratios between the power in the direct path and the power in the scattered paths to the total power in both paths, respectively. Moreover, the capacities of the $\mathcal{S} - \mathcal{R}_m$ and $\mathcal{R}_m - \mathcal{D}$ RF links in the b -th time slot, denoted by $C_{1m}^{\text{rf}}[b]$ and $C_{2m}^{\text{rf}}[b]$, respectively, are given by

$$C_{lm}^{\text{rf}}[b] = W^{\text{rf}} \log_2 \left(1 + \frac{q_{lm}^2[b]}{\delta_{lm}^2} \right), \quad l = 1, 2, \quad (6)$$

where $q_{1m}[b] = \sqrt{P_{\mathcal{S}}^{\text{rf}}} |g_{1m}[b]|$ and $q_{2m}[b] = \sqrt{P_{\mathcal{R}_m}^{\text{rf}}} |g_{2m}[b]|$. Here, $P_{\mathcal{S}}^{\text{rf}}$ and $P_{\mathcal{R}_m}^{\text{rf}}$ are the RF transmit powers of \mathcal{S} and \mathcal{R}_m , respectively.

Remark 1: In this paper, we assume OOK signaling for the FSO links and Gaussian signaling for the RF links. However, we note that the considered problem formulation and the resulting non-BA and BA policies given in the next section are given in general form such that they are also applicable if different signaling schemes are adopted for the RF and FSO links. In particular, for other signaling schemes, only the expressions in (3) and (6) have to be modified and then be used in the proposed relay selection policies presented in Section III.

C. CSI Requirements

In Section III, we derive the optimal non-BA and BA policies assuming that a central node, e.g., the destination, has the instantaneous CSI of all FSO and RF links and is responsible for determining the transmission strategy and conveying it to all other nodes. However, in Subsection IV.B, we present distributed implementations of the optimal policies where each node needs to acquire only the CSI of those RF/FSO links to which it is directly connected. Typically, in hybrid RF/FSO systems, the coherence time of the RF links is on the order of seconds whereas the coherence time of the FSO links is on the order of milliseconds [25]. Therefore, for time slot durations on the order of milliseconds, the hybrid RF/FSO channel is constant and can accommodate thousands of RF/FSO symbols per time slot for typical RF/FSO symbol rates. Because of the large coherence

time, we assume that the signaling overhead caused by channel estimation and feedback is negligible compared to the amount of information transmitted in one time slot.

III. THROUGHPUT-OPTIMAL RELAY SELECTION POLICIES

In this section, we first present the problem formulation for relay selection, and subsequently, we derive the optimal non-BA and BA policies maximizing the throughput as functions of the fading state.

A. Problem Formulation for Relay Selection

For the considered communication system, our goal is to derive optimal relay selection policies which maximize the throughput for both non-BA and BA relays given the CSI of all RF and FSO links. To this end, let $\alpha_{1m}[b]$, $m \in \{1, \dots, M\}$, denote binary selection variables where $\alpha_{1m}[b] = 1$ if relay \mathcal{R}_m is selected for FSO reception in the b -th time slot and $\alpha_{1m}[b] = 0$ if relay \mathcal{R}_m is not selected. Similarly, $\alpha_{2m}[b] = 1$ indicates that relay \mathcal{R}_m is selected for FSO transmission in the b -th time slot and $\alpha_{2m}[b] = 0$ if relay \mathcal{R}_m is not selected. Analogously, $\beta_{1m}[b]$ and $\beta_{2m}[b]$, $m \in \{1, \dots, M\}$, denote binary selection variables for RF relay selection for reception and transmission in the b -th time slot, respectively. For simplicity of implementation, we assume that in each time slot, one relay is selected for RF reception and one relay is selected for FSO reception. Similarly, one relay is selected for RF transmission and one relay is selected for FSO transmission. We note that activation of multiple relay nodes for simultaneous reception or transmission requires more complicated transmission schemes because of the required multi-user encoding/decoding. In addition, it is known that in general, despite its simplicity, relay selection efficiently exploits the diversity gain that independent fading realizations provide [9], [10], [16]. Mathematically, in order to enforce the aforementioned assumptions on the relay selection strategy, $\sum_{\forall m} \alpha_{lm}[b] = 1$, $\forall l, b$, and $\sum_{\forall m} \beta_{lm}[b] = 1$, $\forall l, b$, have to hold.

Due to the broadcast nature of RF, simultaneous activation of the selected relays creates interference from the transmitting relay to the receiving relay. In particular, self-interference occurs if the same relay is selected for both RF transmission and RF reception and inter-relay interference occurs if the relays selected for RF transmission and RF reception are different. Therefore, for the sake of simplicity of implementation and practical feasibility, we assume that the RF links are half duplex with respect to each other. In other words, assuming relays \mathcal{R}_n and $\mathcal{R}_{n'}$ are selected for RF reception and RF transmission, respectively, the $\mathcal{S} - \mathcal{R}_n$ and $\mathcal{R}_{n'} - \mathcal{D}$ RF links cannot be active at the same time. Hence, we activate the $\mathcal{S} - \mathcal{R}_n$ RF link in the $\rho_1[b] \in [0, 1]$ fraction of the b -th time slot and the $\mathcal{R}_{n'} - \mathcal{D}$ RF link in the remaining $\rho_2[b] \in [0, 1]$ fraction of the b -th time slot, respectively, where $\rho_1[b] + \rho_2[b] = 1$, $\forall b$, holds.

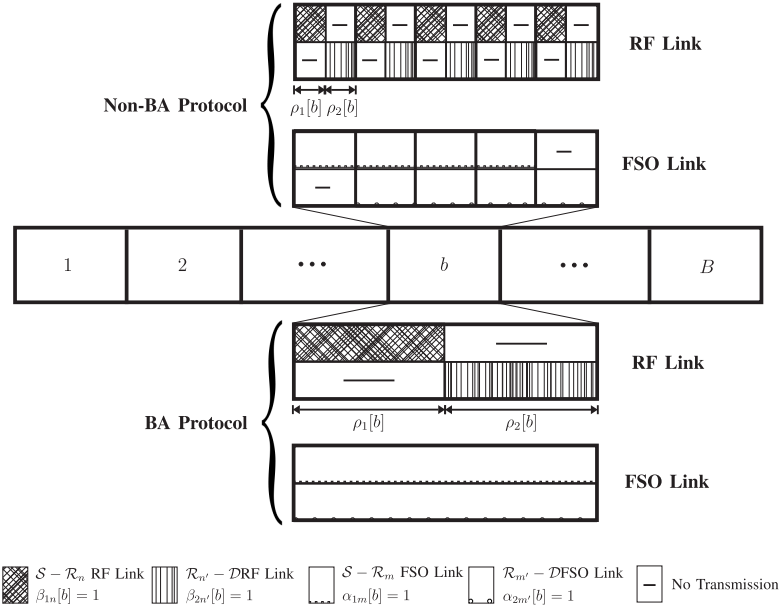


Fig. 2. Proposed transmission protocol for the considered parallel hybrid RF/FSO relay channel.

On the other hand, assuming relays \mathcal{R}_m and $\mathcal{R}_{m'}$ are selected for FSO reception and transmission, respectively, they can simultaneously transmit over both the $\mathcal{S} - \mathcal{R}_m$ and $\mathcal{R}_{m'} - \mathcal{D}$ FSO links, i.e., the FSO links are orthogonal with respect to each other due to narrow-beam property of FSO. In the BA case, the relays can extract data from their buffers and send it to the destination at the same time when they are receiving data from the source. This allows the source and the relays to construct codewords which span one time slot. However, in the non-BA case, if the source codeword spans one time slot, the relays have to wait until the end of the time slot before they can decode the FSO signal. Therefore, the relays cannot forward this data to the destination in the same time slot which contradicts the basic assumption behind non-BA transmission, namely that the data transmitted by the source has to be received by the destination in the same time slot. To alleviate this problem, we assume that for non-BA transmission, each time slot is divided into n sub-slots indexed by $i = 1, 2, \dots, n$. Thereby, the relays can transmit the data received from the source in sub-slot $i = 1, 2, \dots, n - 1$ to the destination in the subsequent sub-slot $i + 1$. Thereby, the effective capacities of the FSO links is $\frac{n-1}{n} C_{lm}^{\text{fso}}[b]$ which approaches $C_{lm}^{\text{fso}}[b]$ as $n \rightarrow \infty$, i.e., the full-duplex property of the FSO links is fully exploited. The considered transmission protocol is schematically illustrated in Fig. 2.

B. Optimal Non-BA Policy

In this subsection, we derive the optimal *adaptive* non-BA RF/FSO relay selection and RF transmission time allocation policies such that the average information rate from the source to

the destination, denoted by $\bar{\tau}$, is maximized. The resulting throughput maximization problem can be formulated as

$$\begin{aligned} & \underset{\alpha \in \mathcal{A}, \beta \in \mathcal{B}, \rho \in \mathcal{C}, \tau \geq 0}{\text{maximize}} && \bar{\tau} = \sum_{\forall m} \bar{\tau}_m = \frac{1}{B} \sum_{\forall b} \sum_{\forall m} \tau_m[b] \\ & \text{subject to} && \tau_m[b] \leq \alpha_{1m}[b] C_{1m}^{\text{fso}}[b] + \beta_{1m}[b] \rho_1[b] C_{1m}^{\text{rf}}[b], \quad \forall m, b, \\ & && \tau_m[b] \leq \alpha_{2m}[b] C_{2m}^{\text{fso}}[b] + \beta_{2m}[b] \rho_2[b] C_{2m}^{\text{rf}}[b], \quad \forall m, b, \end{aligned} \quad (7)$$

where α , β , ρ , and τ are the vectors containing the relay selection variables of the FSO links, the relay selection variables of the RF links, the time sharing variables of the RF links, and the relays' throughputs, respectively. We note that since the optimal non-BA policy depends only on the fading states of the FSO and RF links, and not on the transmission time slot index, we drop the time slot index in this subsection for notational simplicity. Moreover, $\mathcal{A} = \{\alpha | \alpha_{lm} \in \{0, 1\}, \forall l, m \wedge \sum_{\forall m} \alpha_{lm} = 1, \forall l\}$, $\mathcal{B} = \{\beta | \beta_{lm} \in \{0, 1\}, \forall l, m \wedge \sum_{\forall m} \beta_{lm} = 1, \forall l\}$, and $\mathcal{C} = \{\rho | \rho_l \in [0, 1], \forall l \wedge \sum_{\forall l} \rho_l = 1\}$ are the feasible sets of α , β , and ρ , respectively. The constraints in (7) follow from the max-flow min-cut theorem [23], according to which the throughput of relay \mathcal{R}_m is limited by the capacities of the $\mathcal{S} - \mathcal{R}_m$ and $\mathcal{R}_m - \mathcal{D}$ links, respectively. In the following theorem, the optimal solution to the optimization problem in (7) is provided.

Theorem 1: For the parallel non-BA relay channel with hybrid RF/FSO links, the optimal policies for FSO and RF relay selection and optimal RF transmission time allocation are given by

$$\alpha_{lm^*} = \begin{cases} 1, & \text{if } \{\text{Case 1} \wedge m^* = \underset{m}{\text{argmax}} \tau_m^{\text{hyb}}\} \\ \vee \{\text{Case 2} \wedge m^* = \underset{m}{\text{argmax}} \tau_m^{\text{fso}}\} \\ \vee \{\text{Case 3} \wedge l = 1 \wedge (m^*, -) = \underset{(m,n)}{\text{argmax}} \tau_{mn}^{\text{mix}}\} \\ \vee \{\text{Case 3} \wedge l = 2 \wedge (-, m^*) = \underset{(m,n)}{\text{argmax}} \tau_{mn}^{\text{mix}}\} \\ 0, & \text{otherwise} \end{cases} \quad (8a)$$

$$\beta_{lm^*} = \begin{cases} 1, & \text{if } \{\text{Case 1} \wedge m^* = \underset{m}{\text{argmax}} \tau_m^{\text{hyb}}\} \\ \vee \{\text{Case 2} \wedge m^* = \underset{m}{\text{argmax}} \tau_m^{\text{rf}}\} \\ \vee \{\text{Case 3} \wedge l = 1 \wedge (-, m^*) = \underset{(m,n)}{\text{argmax}} \tau_{mn}^{\text{mix}}\} \\ \vee \{\text{Case 3} \wedge l = 2 \wedge (m^*, -) = \underset{(m,n)}{\text{argmax}} \tau_{mn}^{\text{mix}}\} \\ 0, & \text{otherwise} \end{cases} \quad (8b)$$

$$\rho_1^* = 1 - \rho_2^* = \begin{cases} \left[\frac{C_{2m^*}^{\text{fso}} + C_{2m^*}^{\text{rf}} - C_{1m^*}^{\text{fso}}}{C_{1m^*}^{\text{rf}} + C_{2m^*}^{\text{rf}}} \right]_0^1, & \text{if } \{\text{Case 1} \wedge m^* = \underset{m}{\operatorname{argmax}} \tau_m^{\text{hyb}}\} \\ \frac{C_{2m^*}^{\text{rf}}}{C_{1m^*}^{\text{rf}} + C_{2m^*}^{\text{rf}}}, & \text{if } \{\text{Case 2} \wedge m^* = \underset{m}{\operatorname{argmax}} \tau_m^{\text{rf}}\} \\ \frac{C_{2m^*}^{\text{fso}}}{C_{1m^*}^{\text{rf}}}, & \text{if } \{\text{Case 3} \wedge (-, m^*) = \underset{(m,n)}{\operatorname{argmax}} \tau_{mn}^{\text{mix}}\} \end{cases} \quad (8c)$$

where τ_m^{hyb} , τ_{mn}^{ind} , and τ_{mn}^{mix} are given by

$$\tau_m^{\text{hyb}} = \begin{cases} C_{2m}^{\text{fso}} + C_{2m}^{\text{rf}}, & \text{if } \frac{C_{2m}^{\text{fso}} + C_{2m}^{\text{rf}}}{C_{1m}^{\text{fso}}} < 1 \\ C_{1m}^{\text{fso}} + C_{1m}^{\text{rf}}, & \text{if } \frac{C_{1m}^{\text{fso}} + C_{1m}^{\text{rf}}}{C_{2m}^{\text{fso}}} < 1 \\ \frac{C_{2m}^{\text{fso}} + C_{2m}^{\text{rf}} - C_{1m}^{\text{fso}}}{C_{1m}^{\text{rf}} + C_{2m}^{\text{rf}}} C_{1m}^{\text{rf}} + C_{1m}^{\text{fso}}, & \text{otherwise} \end{cases} \quad (9a)$$

$$\tau_{mn}^{\text{ind}} = \tau_m^{\text{fso}} + \tau_n^{\text{rf}}, \text{ where } \begin{cases} \tau_m^{\text{fso}} = \min \{C_{1m}^{\text{fso}}, C_{2m}^{\text{fso}}\} \\ \tau_n^{\text{rf}} = \frac{C_{1n}^{\text{rf}} C_{2n}^{\text{rf}}}{C_{1n}^{\text{rf}} + C_{2n}^{\text{rf}}} \end{cases} \quad (9b)$$

$$\tau_{mn}^{\text{mix}} = \begin{cases} C_{1m}^{\text{fso}} + C_{2n}^{\text{fso}}, & \text{if } \frac{C_{2n}^{\text{fso}}}{C_{1n}^{\text{rf}}} + \frac{C_{1m}^{\text{fso}}}{C_{2m}^{\text{rf}}} \leq 1 \\ 0, & \text{otherwise.} \end{cases} \quad (9c)$$

Moreover, Cases 1-3 are defined as follows

$$\left\{ \begin{array}{l} \text{Case 1 (Hybrid Mode):} \\ \max_m \tau_m^{\text{hyb}} > \max \left\{ \max_m \tau_m^{\text{fso}} + \max_n \tau_n^{\text{rf}}, \max_{(m,n)} \tau_{mn}^{\text{mix}} \right\} \\ \text{Case 2 (Independent Mode):} \\ \max_m \tau_m^{\text{fso}} + \max_n \tau_n^{\text{rf}} > \max \left\{ \max_m \tau_m^{\text{hyb}}, \max_{(m,n)} \tau_{mn}^{\text{mix}} \right\} \\ \text{Case 3 (Mixed Mode):} \\ \max_{(m,n)} \tau_{mn}^{\text{mix}} > \max \left\{ \max_m \tau_m^{\text{hyb}}, \max_m \tau_m^{\text{fso}} + \max_n \tau_n^{\text{rf}} \right\} \end{array} \right. \quad (10)$$

Using the RF and FSO relay selection and RF time allocation policies in (8), the maximum throughput achieved by the protocol in Theorem 1, denoted by τ^* , is given by

$$\tau^* = \begin{cases} \max_m \tau_m^{\text{hyb}} & \text{for Case 1} \\ \max_m \tau_m^{\text{fso}} + \max_n \tau_n^{\text{rf}} & \text{for Case 2} \\ \max_{(m,n)} \tau_{mn}^{\text{mix}} & \text{for Case 3} \end{cases} \quad (11)$$

Proof: Please refer to Appendix A. ■

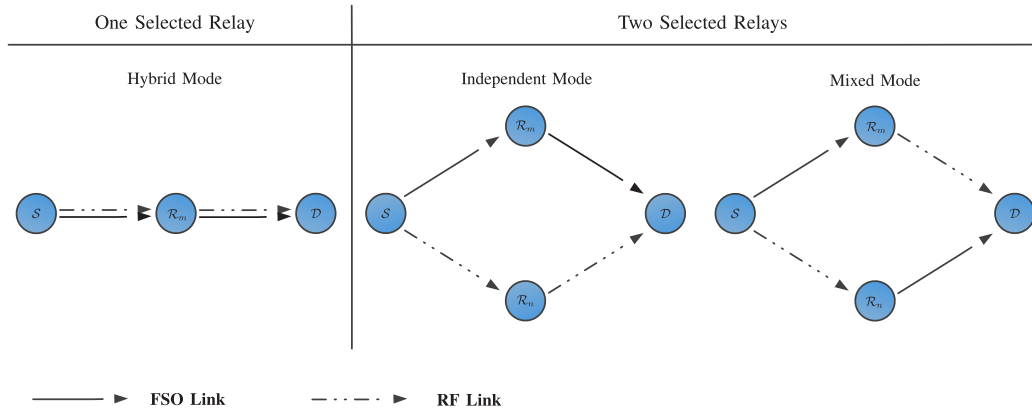


Fig. 3. The three possible optimal non-BA relaying modes in the considered parallel hybrid RF/FSO relay channel.

The feasible sets \mathcal{A} and \mathcal{B} of the relay selection variables allow the selection of at most four different relays for RF/FSO reception and transmission. However, due to the constraints in (7), the optimal relay selection policy selects at most two different relays for RF/FSO reception and transmission in order to ensure that the data which is transmitted from the source to a certain relay can be actually forwarded to the destination. Moreover, the optimal throughput maximizing policy in Theorem 1 reveals that the optimal relay selection policy $(\alpha_{lm}, \beta_{lm})$ belongs to one of the following three cases, see Fig. 3.

Case 1 (Hybrid Mode): The same relay \mathcal{R}_m is selected for FSO/RF transmission/reception, i.e., the RF links serve as support links for the FSO links.

Case 2 (Independent Mode): Relay \mathcal{R}_m is selected for FSO reception and transmission and a different relay \mathcal{R}_n is selected for RF reception and transmission, i.e., the FSO and RF links are used independently.

Case 3 (Mixed Mode): Relays \mathcal{R}_m and \mathcal{R}_n , $m \neq n$, are selected for FSO reception and transmission, respectively, and relays \mathcal{R}_m and \mathcal{R}_n are selected for RF transmission and reception, respectively.

The optimal transmission time allocation to the RF links given in (8c) is found such that the bottleneck throughput of the $\mathcal{S} - \mathcal{R}_m$ and $\mathcal{R}_m - \mathcal{D}$ links is maximized. Thereby, depending on whether \mathcal{R}_m uses both the RF and FSO links, i.e., the hybrid and mixed modes, or only the RF links, i.e., the independent mode, the resulting optimal RF time allocation policy depends on both the RF and FSO fading states or only the RF fading state, respectively.

C. Optimal BA Policy

In this subsection, we assume that the relay nodes take advantage of buffering to transmit/receive in each time slot over the RF/FSO links which have the best qualities. We assume that each relay is equipped with an infinite-size buffer for data storage. Let $Q_m[b]$, $m \in \{1, \dots, M\}$, denote the

amount of information in bits available in the buffer of relay m at the end of the b -th time slot. The dynamics of the queues at the relay nodes can be modelled as

$$Q_m[b] = Q_m[b-1] + \underbrace{\alpha_{1m}[b]C_{1m}^{\text{fso}}[b]}_{R_{1m}^{\text{fso}}[b]} + \underbrace{\beta_{1m}[b]\rho_1[b]C_{1m}^{\text{rf}}[b]}_{R_{1m}^{\text{rf}}[b]} - \underbrace{\min\{Q_m[b-1], \alpha_{2m}[b]C_{2m}^{\text{fso}}[b]\}}_{R_{2m}^{\text{fso}}[b]} \quad (12)$$

$$- \underbrace{\min\left\{[Q_m[b-1] - \alpha_{2m}[b]C_{2m}^{\text{fso}}[b]]^+ + \beta_{1m}[b]\rho_1[b]C_{1m}^{\text{rf}}[b], \beta_{2m}[b]\rho_2[b]C_{2m}^{\text{rf}}[b]\right\}}_{R_{2m}^{\text{rf}}[b]},$$

where $R_{1m}^{\text{fso}}[b]$, $R_{1m}^{\text{rf}}[b]$, $R_{2m}^{\text{fso}}[b]$, and $R_{2m}^{\text{rf}}[b]$ are the data rates of the $\mathcal{S}-\mathcal{R}_m$ FSO, $\mathcal{S}-\mathcal{R}_m$ RF, $\mathcal{R}_m-\mathcal{D}$ FSO, and $\mathcal{R}_m-\mathcal{D}$ RF links, respectively, in the b -th time slot. In particular, at the beginning of each time slot, the amount of data sent over the $\mathcal{R}_m-\mathcal{D}$ FSO link is limited by the capacity of the $\mathcal{R}_m-\mathcal{D}$ FSO link, i.e., $\alpha_{2m}[b]C_{2m}^{\text{fso}}[b]$, and the amount of information available at the relay's buffer, i.e., $Q_m[b-1]$. Similarly, in the second half of the time slot, the amount of data used by relay \mathcal{R}_m to encode the RF codewords is limited by the capacity of the $\mathcal{R}_m-\mathcal{D}$ RF link, i.e., $\beta_{2m}[b]\rho_2[b]C_{2m}^{\text{rf}}[b]$, and the amount of information in the buffer, i.e., $[Q_m[b-1] - \alpha_{2m}[b]C_{2m}^{\text{fso}}[b]]^+ + \beta_{1m}[b]\rho_1[b]C_{1m}^{\text{rf}}[b]$. Since the throughput is equal to the amount of data that is received at the destination, the throughput maximization problem for the BA relaying protocol can be written as

$$\underset{\alpha \in \mathcal{A}, \beta \in \mathcal{B}, \rho \in \mathcal{C}}{\text{maximize}} \quad \bar{\tau} = \sum_{\forall m} \bar{\tau}_m = \sum_{\forall m} [R_{2m}^{\text{fso}}[b] + R_{2m}^{\text{rf}}[b]]. \quad (13)$$

Solving the above optimization problem is quite involved due to recursive dynamics of the queue (12) which appear in $R_{2m}^{\text{fso}}[b]$ and $R_{2m}^{\text{rf}}[b]$. To tackle this problem, we use a useful result from queuing theory [26, Chapter 2], [27, Eq. (50)]. Suppose $A[b]$, $D[b]$, $C[b]$, and $Q[b]$ are the arrival rate, the departure rate, the processing rate (departure capacity), and the amount of information of a queue in the b -th time slot, respectively. Thereby, although the *instantaneous* departure rate of the queue is limited by the amount of data available at the queue, i.e., $D[b] = \min\{Q[b], C[b]\}$, the *average* departure rate can be written independent of the dynamics of the queue as $\mathbb{E}\{D\} = \min\{\mathbb{E}\{A\}, \mathbb{E}\{C\}\}$, see [27, Appendix E] for a detailed proof. Using this result and as $B \rightarrow \infty$, the throughput maximizing policy for this case can be obtained by solving the following optimization problem

$$\underset{\alpha \in \mathcal{A}, \beta \in \mathcal{B}, \rho \in \mathcal{C}, \tau \geq 0}{\text{maximize}} \quad \bar{\tau} = \sum_{\forall m} \bar{\tau}_m \quad (14)$$

$$\text{subject to} \quad \bar{\tau}_m \leq \frac{1}{B} \sum_{\forall b} [\alpha_{1m}[b]C_{1m}^{\text{fso}}[b] + \beta_{1m}[b]\rho_1[b]C_{1m}^{\text{rf}}[b]], \quad \forall m,$$

$$\bar{\tau}_m \leq \frac{1}{B} \sum_{\forall b} [\alpha_{2m}[b]C_{2m}^{\text{fso}}[b] + \beta_{2m}[b]\rho_2[b]C_{2m}^{\text{rf}}[b]], \quad \forall m,$$

where the right-hand sides of the first and second constraints are the average arrival rate and the average departure capacity of the queue at \mathcal{R}_m , respectively.

As can be observed from the constraints in (14), for BA relaying, the *average* throughput of each relay is limited. In contrast, for non-BA relaying, cf. (7), the *instantaneous* throughput of each relay is limited. Therefore, the feasible set of the problem in (14) is larger than that of (7) which leads to a higher achievable throughput for the BA relaying protocol. The higher achievable throughput of the BA protocol comes at the expense of an increased end-to-end delay. Hence, the BA protocol is a suitable option for delay-tolerant applications. In the following theorem, we present the optimal BA relay selection policy as the solution of the problem in (14). For notational simplicity, let $C_{lm}^{\text{fso}}(h_{lm})$ and $C_{lm}^{\text{rf}}(g_{lm})$ denote the capacities of the FSO and RF links as functions of the fading states, respectively. Moreover, $f_{\mathbf{h}_l}(\mathbf{h}_l)$ and $f_{\mathbf{g}_l}(\mathbf{g}_l)$, $l = 1, 2$, denote the pdfs of the random vectors \mathbf{h}_l and \mathbf{g}_l , respectively, where \mathbf{h}_l and \mathbf{g}_l are the vectors containing the fading coefficients of the l -th hop of the FSO links and the RF links, respectively. Furthermore, we introduce constant vector $\boldsymbol{\lambda} = [\lambda_1, \lambda_2, \dots, \lambda_M]$ which we will use for the statement of the optimal protocol. The elements of vector $\boldsymbol{\lambda}$ are in fact related to the Lagrange multipliers corresponding to the constraints in (14).

Theorem 2: For the parallel BA relay channel with hybrid RF/FSO links, the optimal policies for FSO and RF relay selection and optimal RF transmission time allocation as a function of the fading state are given by

$$\alpha_{lm^*}(\mathbf{h}_l) = \begin{cases} 1, & \text{if } m^* = \operatorname{argmax}_m \Lambda_{lm}^{\text{fso}}(h_{lm}) \\ 0, & \text{otherwise,} \end{cases} \quad (15a)$$

$$\beta_{lm^*}(\mathbf{g}_1, \mathbf{g}_2) = \begin{cases} 1, & \text{if } m^* = \operatorname{argmax}_{l,m} \Lambda_{lm}^{\text{rf}}(g_{lm}) \\ 0, & \text{otherwise,} \end{cases} \quad (15b)$$

$$\rho_{l^*}(\mathbf{g}_1, \mathbf{g}_2) = \begin{cases} 1, & \text{if } l^* = \operatorname{argmax}_{l,m} \Lambda_{lm}^{\text{rf}}(g_{lm}) \\ 0, & \text{otherwise,} \end{cases} \quad (15c)$$

where $\Lambda_{1m}^{\text{fso}}(h_{1m}) = \lambda_m C_{1m}^{\text{fso}}(h_{1m})$, $\Lambda_{2m}^{\text{fso}}(h_{2m}) = (1 - \lambda_m) C_{2m}^{\text{fso}}(h_{2m})$, $\Lambda_{1m}^{\text{rf}}(g_{1m}) = \lambda_m C_{1m}^{\text{rf}}(g_{1m})$, and $\Lambda_{2m}^{\text{rf}}(g_{2m}) = (1 - \lambda_m) C_{2m}^{\text{rf}}(g_{2m})$. In addition, λ_m is a constant which depends on the fading distributions $f_{\mathbf{h}_l}(\mathbf{h}_l)$ and $f_{\mathbf{g}_l}(\mathbf{g}_l)$. The optimal value of λ_m can be obtained offline before transmission starts using an iterative algorithm with the following update equation in the k -th iteration

$$\lambda_m[k+1] = \left[\lambda_m[k] - \epsilon_m[k] \left(\bar{C}_{1m}^{\text{fso}}[k] + \bar{C}_{1m}^{\text{rf}}[k] - \bar{C}_{2m}^{\text{fso}}[k] - \bar{C}_{2m}^{\text{rf}}[k] \right) \right]_0^1, \quad (16)$$

where $\epsilon_m[k]$, $\forall m$, is a sufficiently small step size. Moreover, the average capacity terms, $\bar{C}_{lm}^{\text{fso}}[k]$ and $\bar{C}_{lm}^{\text{rf}}[k]$, are given by

$$\bar{C}_{lm}^{\text{fso}}[k] = \mathbb{E} \{ \alpha_{lm^*}(\mathbf{h}_l) C_{lm}^{\text{fso}}(h_{lm}) \} = \int_{\mathbf{h}_l} \alpha_{lm^*}(\mathbf{h}_l) C_{lm}^{\text{fso}}(h_{lm}) f_{\mathbf{h}_l}(\mathbf{h}_l) d\mathbf{h}_l, \quad l = 1, 2, \quad (17a)$$

$$\begin{aligned} \bar{C}_{lm}^{\text{rf}}[k] &= \mathbb{E} \{ \beta_{lm^*}(\mathbf{g}_1, \mathbf{g}_2) \rho_{l^*}(\mathbf{g}_1, \mathbf{g}_2) C_{lm}^{\text{rf}}(g_{lm}) \} \\ &= \iint_{\mathbf{g}_1, \mathbf{g}_2} \beta_{lm^*}(\mathbf{g}_1, \mathbf{g}_2) \rho_{l^*}(\mathbf{g}_1, \mathbf{g}_2) C_{lm}^{\text{rf}}(g_{lm}) f_{\mathbf{g}_1}(\mathbf{g}_1) f_{\mathbf{g}_2}(\mathbf{g}_2) d\mathbf{g}_1 d\mathbf{g}_2, \quad l = 1, 2, \end{aligned} \quad (17b)$$

where $\alpha_{lm^*}(\mathbf{h}_l)$, $\beta_{lm^*}(\mathbf{g}_1, \mathbf{g}_2)$, and $\rho_{l^*}(\mathbf{g}_1, \mathbf{g}_2)$ are given by (15) with $\lambda_m = \lambda_m[k]$. Substituting the optimal FSO and RF relay selection and RF time allocation variables from (15) and the optimal λ^* from (16) into (17), the maximum throughput is obtained as

$$\bar{\tau}^* = \sum_m \bar{\tau}_m^* = \sum_m \min \{ \bar{C}_{1m}^{\text{fso}} + \bar{C}_{1m}^{\text{rf}}, \bar{C}_{2m}^{\text{fso}} + \bar{C}_{2m}^{\text{rf}} \}. \quad (18)$$

Proof: Please refer to Appendix B. ■

Recall that the optimal non-BA protocol in Theorem 1 selects at most two different relays for RF/FSO reception and transmission. On the other hand, exploiting the buffering capability of the relay nodes and the degrees of freedom available in the feasible sets \mathcal{A} and \mathcal{B} , the BA protocol may select up to four different relays for RF/FSO reception and transmission in one time slot because the relays are not forced to immediately forward the information received from the source to the destination. However, Theorem 2 reveals that it is optimal to select at most three different relays, namely two relays for FSO reception and transmission and one relay for either RF reception or transmission. The selection of only one relay for the RF links leads to binary values for the RF time allocation variable in (15c), i.e., RF time allocation reduces to RF link selection. Moreover, based on the number of relays selected by the optimal BA protocol, there are ten possible transmission modes which are illustrated in Fig. 4. These ten transmission modes can be further categorized into the following three types. *i) Hybrid Modes:* The RF link is used as backup for one of the FSO links. *ii) Independent Modes:* None of the relays uses both RF and FSO links. *iii) Mixed Modes:* The RF link is cascaded with one of the FSO links.

Remark 2: In the optimal non-BA protocol, the values of α_{lm} , β_{lm} , and ρ_l depend on the fading states of both the RF and FSO links in the network. In contrast, in the optimal BA protocol, $\alpha_{lm}(\mathbf{h}_l)$ is only a function of the instantaneous CSI of the FSO links and not of the instantaneous CSI of the RF links. Similarly, $\beta_{lm}(\mathbf{g}_1, \mathbf{g}_2)$ and $\rho_l(\mathbf{g}_1, \mathbf{g}_2)$ are only functions of the instantaneous CSI of the RF links and not of the instantaneous CSI of the FSO links. In particular, by comparing the $\Lambda_{1m}^{\text{fso}}(h_{1m})$ for all the $\mathcal{S} - \mathcal{R}_m$ FSO links, one relay is selected for FSO reception in (15a), by comparing the

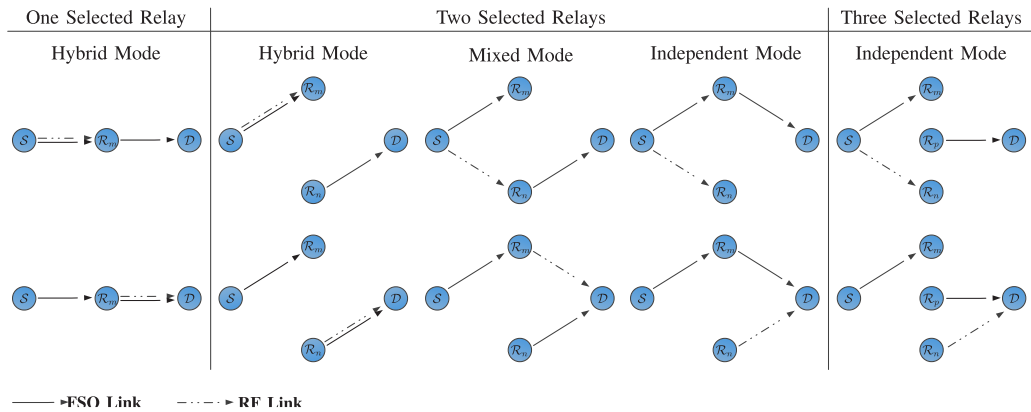


Fig. 4. The ten possible optimal BA relaying modes in the considered parallel hybrid RF/FSO relay channel.

$\Lambda_{2m}^{\text{fso}}(h_{2m})$ for all the $\mathcal{R}_m - \mathcal{D}$ FSO links, one relay is selected for FSO transmission in (15a), and by comparing the $\Lambda_{1m}^{\text{rf}}(g_{1m})$ and $\Lambda_{2m}^{\text{rf}}(g_{2m})$ for all the RF links, one relay is selected for either RF reception or RF transmission in (15b,c). We note that although the optimal $\alpha_{lm}(\mathbf{h}_l)$ ($\beta_{lm}(\mathbf{g}_1, \mathbf{g}_2) / \rho_l(\mathbf{g}_1, \mathbf{g}_2)$) does not depend on the instantaneous CSI of the RF (FSO) links, the statistical CSI of the RF (FSO) links does affect $\alpha_{lm}(\mathbf{h}_l)$ ($\beta_{lm}(\mathbf{g}_1, \mathbf{g}_2) / \rho_l(\mathbf{g}_1, \mathbf{g}_2)$) through Lagrange multiplier λ , cf. (16) and (17).

IV. PRACTICAL CHALLENGES OF THE OPTIMAL PROTOCOLS

In this section, we investigate two practical challenges of the optimal protocols, namely the unbounded end-to-end delay of the optimal BA protocol and the global CSI requirement of both the optimal non-BA and BA policies. To cope with these challenges, we first modify the optimal delay-unconstrained BA policy given in Theorem 2 to obtain a delay-constrained BA policy. Subsequently, we present distributed implementations for both the optimal non-BA and BA protocols proposed in Theorem 1 and Theorem 2, respectively, which require only local CSI knowledge at each node.

A. Delay-Constrained BA Policy

In the non-BA protocol, the relay nodes are forced to immediately forward the data received from the source to the destination. Therefore, the non-BA protocol is an appropriate option for applications with stringent delay requirements. On the other hand, in the BA protocol, the relay nodes are allowed to store the data received from the source in their buffers and forward it to the destination when the quality of the relay-destination links is favorable. This leads to an improvement of the throughput at the expense of an increased end-to-end delay. In fact, since there is no limitation on the delay caused by the optimal BA protocol, its end-to-end delay may become unbounded. However, for most practical applications, it is necessary that the delay remains within a certain range. In the

following, we show that a small modification of the optimal BA protocol in Theorem 2 leads to a delay-constrained protocol whose throughput approaches that of the delay-unconstrained protocol even for small target average delays.

For the development of the proposed delay-constrained protocol, we limit the size of the buffer at the m -th relay to Q_m^{\max} , $m \in \{1, \dots, M\}$. Due to the limited buffer size, the transmit rate of the source to relay m in the b -th time slot, denoted by $R_{1m}[b]$, is not only limited by the capacities of the $\mathcal{S} - \mathcal{R}_m$ RF and FSO links, i.e., $C_{1m}^{\text{rf}}[b]$ and $C_{1m}^{\text{fso}}[b]$, but also by the amount of space available in the buffer of the m -th relay, i.e., $Q_m^{\max} - Q_m[b - 1]$. Similarly, the rate at which the relay transmits to the destination in the b -th time slot, denoted by $R_{2m}[b]$, is not only limited by the capacities of the $\mathcal{R}_m - \mathcal{D}$ RF and FSO links, i.e., $C_{2m}^{\text{rf}}[b]$ and $C_{2m}^{\text{fso}}[b]$, but also by the amount of information available in the buffer of the m -th relay, i.e., $Q_m[b - 1]$. In the following, we present the proposed delay-constrained BA policy.

Proposed Delay-Constrained BA Policy: For the parallel BA relay channel with hybrid RF/FSO links, the policies for FSO and RF relay selection and optimal RF transmission time allocation given by (15) in Theorem 2 lead to a constrained average end-to-end delay if the following modified selection metrics are employed

$$\tilde{\Lambda}_{1m}^{\text{fso}}[b] = \lambda_m \min \{ C_{1m}^{\text{fso}}[b], Q_m^{\max} - Q_m[b - 1] \} \quad (19a)$$

$$\tilde{\Lambda}_{2m}^{\text{fso}}[b] = (1 - \lambda_m) \min \{ C_{2m}^{\text{fso}}[b], Q_m[b - 1] \} \quad (19b)$$

$$\tilde{\Lambda}_{1m}^{\text{rf}}[b] = \lambda_m \min \{ C_{1m}^{\text{rf}}[b], Q_m^{\max} - Q_m[b - 1] \} \quad (19c)$$

$$\tilde{\Lambda}_{2m}^{\text{rf}}[b] = (1 - \lambda_m) \min \{ C_{2m}^{\text{rf}}[b], Q_m[b - 1] \}, \quad (19d)$$

where λ_m , $m \in \{1, \dots, M\}$, is obtained from (16) in Theorem 2. Moreover, considering that the optimal values of $\rho_l[b]$ are binary in (15c), the dynamics of the queue can be simplified with respect to (12) so that $Q_m[b]$ is updated in the b -th time slot according to

$$\begin{aligned} Q_m[b] = & Q_m[b - 1] - \min \{ \alpha_{2m}[b] C_{2m}^{\text{fso}}[b] + \beta_{2m}[b] \rho_2[b] C_{2m}^{\text{rf}}[b], Q_m[b - 1] \} \\ & + \min \{ \alpha_{1m}[b] C_{1m}^{\text{fso}}[b] + \beta_{1m}[b] \rho_1[b] C_{1m}^{\text{rf}}[b], Q_m^{\max} - Q_m[b - 1] \}. \end{aligned} \quad (20)$$

Furthermore, the average throughput of the proposed delay-constrained protocol is obtained as

$$\begin{aligned} \bar{\tau} = & \sum_m \bar{\tau}_m = \frac{1}{B} \sum_m \sum_b R_{2m}[b] \\ = & \frac{1}{B} \sum_m \sum_b \min \{ \alpha_{2m}[b] C_{2m}^{\text{fso}}[b] + \beta_{2m}[b] \rho_2[b] C_{2m}^{\text{rf}}[b], Q_m[b - 1] \}. \end{aligned} \quad (21)$$

Average Delay: The average delay of the proposed protocol is calculated as follows. Let $T[b]$ denote the waiting time (delay) that a bit transmitted by the source in the b -th time slot experiences until it reaches the destination. In other words, if a bit is transmitted in the b -th time slot by the source and is decoded in the b' -th time slot by the destination, the delay for this bit is $T[b] = b' - b$ time slots. Thereby, according to Little's Law [28], the average waiting time/delay of all data transmitted by the source, denoted by \bar{T} , is given by

$$\bar{T} = \frac{\sum_{m=1}^M \mathbb{E} \{Q_m[b]\}}{\sum_{m=1}^M \mathbb{E} \{R_{1m}[b]\}}, \quad (22)$$

where $Q_m[b]$ is given in (20) and $R_{1m}[b]$ is given by

$$R_{1m}[b] = \min \{ \alpha_{1m}[b] C_{1m}^{\text{fso}}[b] + \beta_{1m}[b] \rho_1[b] C_{1m}^{\text{rf}}[b], Q_m^{\text{max}} - Q_m[b-1] \}. \quad (23)$$

Remark 3: The proposed delay-constrained protocol is able to efficiently limit the average delay by considering not only the instantaneous RF and FSO channel qualities for relay selection and RF time allocation but also the status of the buffers at the relays, cf. (19). Thereby, the smaller the maximum buffer size, i.e., Q_m^{max} , the smaller the average delay, i.e., \bar{T} . We note that the proposed delay-constrained protocol is *heuristic*. In fact, even for the simple three-node RF relay channel, the optimal policy which maximizes the average throughput for a given average delay is not known [29]. However, we show in Section V that the proposed heuristic protocol is quite efficient such that for small average delays, e.g. 20 time slots, it achieves a throughput close to that of the optimal delay-unconstrained protocol in Theorem 2.

B. Distributed Implementation

The optimal protocols in Theorem 1 and Theorem 2 require global CSI knowledge. On the other hand, relay selection protocols which do not require global CSI knowledge have been proposed in the literature, see e.g. [18], [29], [30]. In particular, for pure RF communications, the distributed implementation of relay selection based on the use of synchronized timers was proposed in [30] for non-BA relay selection and in [29] for BA relay selection. In the following, we present distributed implementations for the non-BA and BA protocols proposed in Theorem 1 and Theorem 2, respectively. For distributed implementation of the proposed non-BA and BA protocols, each relay node is required to know only the CSI of the FSO and RF links it is connected to.

1) *Distributed Implementation of the Optimal Non-BA Protocol:* For the optimal non-BA protocol, the proposed distributed implementation involves the following four phases.

Phase I:) At the beginning of each time slot, source and destination send pilots to the relay nodes.

Then, the relays estimate the CSI of their respective FSO and RF channels.

Phase II:) To identify the optimal mode, i.e., the hybrid, independent, or mixed mode, each relay has to locally compute the following five throughputs: the throughput of the hybrid mode, τ_m^{hyb} , using (9a); the throughput of the involved FSO links, τ_m^{fso} , using (9b); the throughput of the involved RF links, τ_m^{rf} , using (9b); and the throughputs $\tau_m^{\text{mix1}} = \min\{C_{1m}^{\text{fso}}, C_{2m}^{\text{rf}}\}$ and $\tau_m^{\text{mix2}} = \min\{C_{1m}^{\text{rf}}, C_{2m}^{\text{fso}}\}$. Note that these five throughputs can be calculated at each relay node based on the CSI of the FSO and RF links to which it is directly connected.

Phase III:) Each relay sets five timers T_m^{hyb} , T_m^{fso} , T_m^{rf} , T_m^{mix1} , and T_m^{mix2} which expire after η/τ_m^{hyb} , η/τ_m^{fso} , η/τ_m^{rf} , $\eta/\tau_m^{\text{mix1}}$, and $\eta/\tau_m^{\text{mix2}}$ seconds, respectively, where η is a constant which scales the expiry time into a reasonable range. For each $\zeta \in \{\text{hyb}, \text{fso}, \text{rf}, \text{mix1}, \text{mix2}\}$, the relay whose timer T_m^ζ expires first broadcasts beacon B_m^ζ which contains the information of the relay index m and the timer index ζ . At the same time, all relay nodes listen and if they receive beacon B_m^ζ , $\zeta \in \{\text{hyb}, \text{fso}, \text{rf}, \text{mix1}, \text{mix2}\}$, from another relay, they do not emit their own beacon B_m^ζ .

Phase IV:) After transmission of the beacons, all the nodes decode the information of each transmitted beacon and determine the index of the relays with maximum τ_m^ζ , $\forall \zeta$. Moreover, by measuring the expiry time of the timers which expired first, all the nodes can calculate the corresponding maximum throughput for each ζ as $\max_m \tau_m^\zeta = \eta/T_m^\zeta$. Hence, the nodes are able to calculate the maximum throughputs of the hybrid mode, $\max_m \tau_m^{\text{hyb}}$, the independent mode, $\max_m \tau_m^{\text{fso}} + \max_m \tau_m^{\text{rf}}$, and the mixed mode, $\max_m \tau_m^{\text{mix1}} + \max_m \tau_m^{\text{mix2}}$, and can distributedly determine the optimal mode as the one with the maximum throughput among the candidate hybrid, independent, and mixed modes and the corresponding optimal RF/FSO relays.

2) *Distributed Implementation of the Optimal BA Protocol:* The proposed distributed implementation of the optimal BA protocol involves four phases as follows.

Phase I:) At the beginning of each time slot, source and destination transmit pilots to the relay nodes. Then, the relays estimate the CSI of their respective FSO and RF channels.

Phase II:) To select the best relays, each relay has to compute its respective selection metrics given in Theorem 2, i.e., $\Lambda_{lm}^{\text{fso}}(h_{lm})$ and $\Lambda_{lm}^{\text{rf}}(g_{lm})$, $l = 1, 2$, as follows. Each relay calculates the capacities of its respective FSO and RF links, i.e., $C_{lm}^{\text{fso}}[b]$ and $C_{lm}^{\text{rf}}[b]$, $l = 1, 2$, using (3) and (6), respectively. Moreover, λ_m is a constant and can be obtained offline at the beginning of the transmission process using (16). Using λ_m and the capacities of the involved RF and FSO links, each relay is able to calculate its respective selection metrics in each time slot.

Phase III:) Each relay sets three timers T_m^{fso1} , T_m^{fso2} , and T_m^{rf} which expire after $\eta/\Lambda_{1m}^{\text{fso}}(h_{1m})$, $\eta/\Lambda_{2m}^{\text{fso}}(h_{2m})$, and $\eta/\max\{\Lambda_{1m}^{\text{rf}}(g_{1m}), \Lambda_{2m}^{\text{rf}}(g_{2m})\}$ seconds, respectively. For the FSO links, for each $\xi \in \{\text{fso1}, \text{fso2}\}$, the relay whose timer T_m^ξ expires first broadcasts beacon B_m^ξ . For the RF links, the

relay whose timer T_m^{rf} expires first broadcasts beacon B_m^{rf1} if $\max\{\Lambda_{1m}^{\text{rf}}(g_{1m}), \Lambda_{2m}^{\text{rf}}(g_{2m})\} = \Lambda_{1m}^{\text{rf}}(g_{1m})$ and beacon B_m^{rf2} if $\max\{\Lambda_{1m}^{\text{rf}}(g_{1m}), \Lambda_{2m}^{\text{rf}}(g_{2m})\} = \Lambda_{2m}^{\text{rf}}(g_{2m})$. The beacons contain information about the relay index m and whether the relay is selected for RF/FSO reception or RF/FSO transmission. **Phase IV:**) The nodes which transmit beacons are the selected relays. Hence, after transmission and reception of the beacons, each node knows which relays are selected for RF/FSO reception and transmission.

V. SIMULATION RESULTS

In this section, we first present benchmark schemes for the proposed relay selection policies. Subsequently, we evaluate the performances of the proposed protocols and compare them with those of the benchmark schemes.

A. Benchmark Schemes

As benchmark scheme for the non-BA protocol, we consider the well-known max-min relay selection protocol [9], [30] where for each fading state, the relay with the maximum bottleneck capacity, i.e., the minimum of the capacities of the $\mathcal{S} - \mathcal{R}_m$ and $\mathcal{R}_m - \mathcal{D}$ links, is selected. A recent overview of BA relay selection protocols is provided in [18]. For the BA case, we select the scheme in [29] as benchmark scheme for the proposed BA protocol where, in each time slot, the optimal relay is selected such that the end-to-end throughput is maximized. We note that the protocol in [29] outperforms the other BA protocols available in the literature including the max-max protocol in [19] and the max-link protocol in [20] in terms of the achievable rate.

More in detail, we employ the protocols in [29] and [30] for the following two scenarios: *i) FSO only:* Relay selection for the FSO links without RF links as backups [8], [9] and *ii) Independent RF/FSO relay selection:* Relay selection and data transmission are performed independently for the RF and FSO links. In the non-BA benchmark schemes, we assume that for the RF links, each time slot is divided into two sub-time slots of equal length for $\mathcal{S} - \mathcal{R}_m$ and $\mathcal{R}_m - \mathcal{D}$ RF transmission. We compare the proposed protocols with the FSO-only protocols to quantify the performance gain introduced by RF backup links. Moreover, we consider the independent RF/FSO protocol to evaluate the benefits of the proposed optimal transmission strategies in hybrid RF/FSO systems.

B. Performance Evaluation

Unless otherwise stated, the values of the parameters for the RF and FSO links used to produce the simulation results reported in this section are given in Table I. In particular, we generated random fading realizations for $B = 10^5$ time slots, applied the proposed and the benchmark relay selection

TABLE I
DEFAULT VALUES FOR SYSTEM PARAMETERS [12], [21].

RF Link		FSO Link	
Parameter	Value	Parameter	Value
G_{tx}^{rf}, G_{rx}^{rf}	10 dBi	R	$0.5 \frac{1}{T}$
P_S^{rf}, P_R^{rf}	0.2 mW (23 dBm)	P_S^{fso}, P_R^{fso}	20 mW (13 dBm)
N_0	-114 dBm/MHz	σ^2	$10^{-14} A^2$
λ^{rf}	85.7 mm (3.5 GHz)	λ^{fso}	1550 nm (193 THz)
W^{rf}	20 MHz	W^{fso}	1 GHz
(Ω, Ψ)	(4, 1)	(Θ, Φ)	(2.23, 1.54)
ν	3.5	k	0.032 (light-moderate fog)
N_F	5 dB	r	10 cm
d_{ref}^{rf}	80 m	ϕ	2 mrad

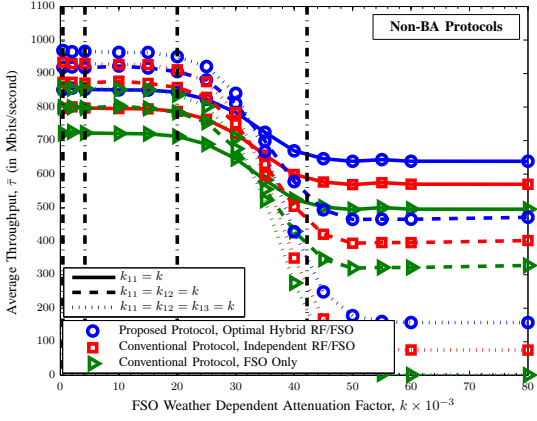


Fig. 5. Average throughput, $\bar{\tau}$, in Mbits/second vs. FSO weather-dependent attenuation factor, $k \times 10^{-3}$, for $M = 3$ and $d_{1m} = d_{2m} = 800$ m (non-BA case). From low to high values of k , the vertical dashed-dotted lines represent the following weather conditions [12]: clear air, haze, light fog, and moderate fog, respectively.

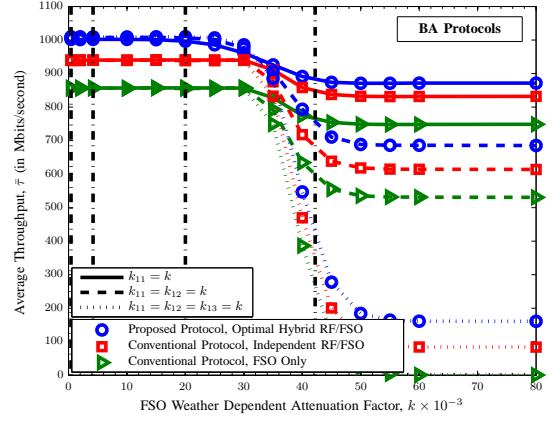


Fig. 6. Average throughput, $\bar{\tau}$, in Mbits/second vs. FSO weather-dependent attenuation factor, $k \times 10^{-3}$, for $M = 3$ and $d_{1m} = d_{2m} = 800$ m (BA case). From low to high values of k , the vertical dashed-dotted lines represent the following weather conditions [12]: clear air, haze, light fog, and moderate fog, respectively.

policies in each time slot, and computed the throughput for each policy as the average data rate received at the destination using that policy.

In Figs. 5 and 6, we show the average throughput vs. the weather-dependent attenuation factor of the FSO links, k , for the non-BA and BA protocols, respectively. We assume $M = 3$, $d_{1m} = d_{2m} = 800$ m, and consider the following three scenarios. In the first scenario, we vary only $k_{11} = k$; in the second scenario, we vary $k_{11} = k_{12} = k$; and in the third scenario, we vary $k_{11} = k_{12} = k_{13} = k$, i.e., the weather-dependent attenuation factors of all FSO links in the first hop. The considered scenarios reflect the fact that different FSO links may be affected by different weather conditions, e.g. passing clouds or birds may affect only some of the FSO links. From Figs. 5 and 6, we observe that the throughput decreases as k increases. Moreover, as $k \rightarrow \infty$, all throughputs saturate at certain values representing the case where the corresponding FSO links are not available anymore. For instance, for the FSO-only protocol in the third scenario, the throughput drops to zero as $k \rightarrow \infty$ since all the FSO links of the first hop become unavailable. In contrast, the proposed protocol achieves a

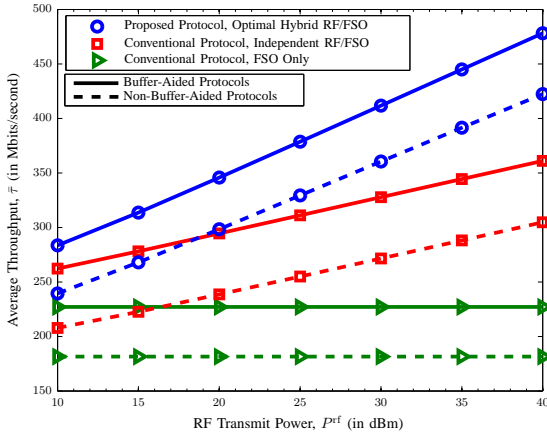


Fig. 7. Average throughput, $\bar{\tau}$, in Mbits/second vs. RF transmit power, $P_S^{\text{rf}} = P_R^{\text{rf}} = P^{\text{rf}}$, for $M = 3$, $d_{1m} = 1000$ m, and $d_{2m} = 800$ m.

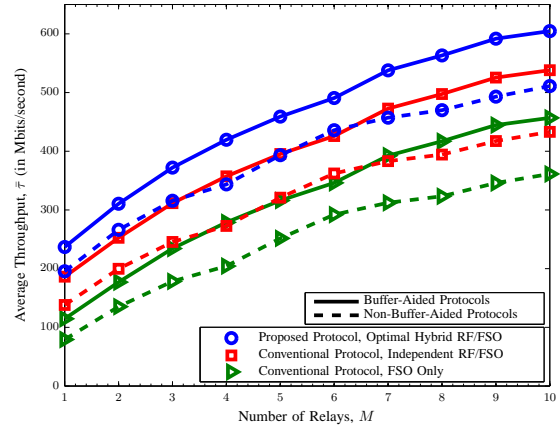


Fig. 8. Average throughput, $\bar{\tau}$, in Mbits/second vs. number of relays, M , for $d_{1m} = 1000$ m and $d_{2m} = 800$ m.

non-zero throughput because of the RF back-up links and outperforms the independent RF/FSO protocol. Furthermore, by comparing the curves in Figs. 5 and 6, we observe that the BA protocols achieve higher throughputs than the corresponding non-BA protocols.

In Fig. 7, the average throughput vs. the RF transmit power is shown for $M = 3$, $d_{1m} = 1000$ m, and $d_{2m} = 800$ m for both non-BA and BA relays. As can be seen from Fig. 7, the average throughputs of the independent RF/FSO protocols and the proposed protocols increase with increasing RF transmit power whereas the throughputs of the FSO-only protocols do not depend on the RF transmit power. Moreover, due to optimal joint relay selection for the RF and FSO links, the proposed protocols not only outperform the independent RF/FSO protocols for both the non-BA and the BA cases but also achieve a higher multiplexing gain for the considered range of RF transmit powers. Furthermore, as expected, the BA protocols considerably outperform the non-BA protocols.

In Fig. 8, we show the average throughput vs. the number of relay nodes for $d_{1m} = 1000$ m and $d_{2m} = 800$ m for both non-BA and BA relays. From this figure, we observe that by increasing the number of relays, the throughput can be considerably improved due to the available spatial diversity. For instance, for the proposed BA protocol, we observe throughput improvements of 95% and 150% for $M = 5$ and $M = 10$, respectively, compared to the case of $M = 1$. Fig. 8 also confirms that the proposed protocols outperform all considered benchmark schemes by a large margin.

Recall that the gains that the BA protocols achieve compared to the non-BA protocols come at the expense of an unbounded end-to-end delay. Therefore, in Fig. 9, we study the performance of the delay-constrained BA protocol developed in Subsection IV.A. In particular, in Fig. 9, we show the average throughput vs. the average delay for $M \in \{1, 3, 5\}$ and $d_{1m} = d_{2m} = 800$ m. For each point on the curves for the proposed delay-constrained BA protocol, we chose an appropriate value

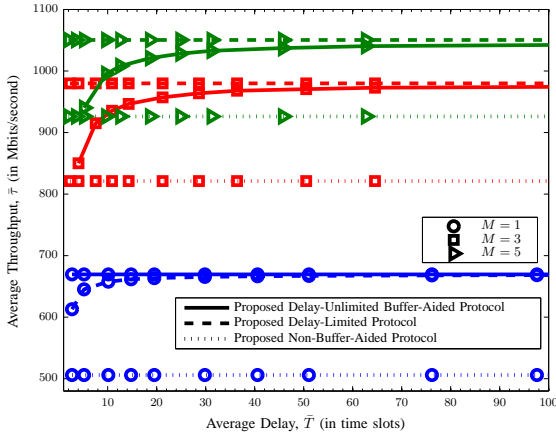


Fig. 9. Average throughput, $\bar{\tau}$, in Mbits/second vs. average delay, \bar{T} , for $M \in \{1, 3, 5\}$ and $d_{1m} = d_{2m} = 800$ m.

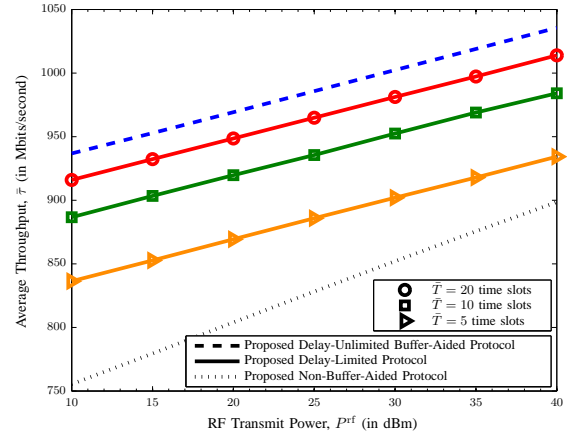


Fig. 10. Average throughput, $\bar{\tau}$, in Mbits/second vs. RF transmit power, $P_S^{\text{rf}} = P_R^{\text{rf}} = P^{\text{rf}}$, for $M = 3$ and $d_{1m} = d_{2m} = 800$ m.

for Q^{\max} which led to the desired delay. Additionally, Fig. 9 includes results for the non-BA and the delay-unconstrained BA protocols as lower and upper bounds for the throughput with average delays of $\bar{T} \leq 1$ and $\bar{T} \rightarrow \infty$ time slots, respectively. We observe that for sufficiently large target average delays, the throughput of the delay-constrained protocol approaches the delay-unconstrained upper bound which reveals the effectiveness of the proposed delay-constrained protocol.

To further investigate the performance of the proposed delay-constrained protocol, in Fig. 10, we plot the average throughput vs. the RF transmit power for $M = 3$ and $d_{1m} = d_{2m} = 800$ m for delays of $\bar{T} \in \{5, 10, 20\}$ time slots. Fig. 10 reveals that as the allowed delay increases, the achievable throughput improves. Furthermore, for a delay of 20 time slots, the proposed delay-constrained protocol significantly outperforms the non-BA protocol and achieves an average throughput close to the upper bound for the considered range of RF transmit powers.

VI. CONCLUSIONS

We investigated the problem of throughput maximization for the parallel hybrid RF/FSO relay channel. Thereby, we distinguished two cases depending on whether or not the relays are equipped with buffers. For both cases, we derived the optimal relay selection policies for transmission and reception for the RF and FSO links and the optimal time allocation policies for RF transmission and reception. Additionally, since the optimal BA policy introduces unbounded delay, we proposed a delay-constrained BA policy which ensures a certain target average end-to-end delay. Furthermore, we developed distributed implementations of the proposed optimal non-BA and BA policies. Simulation results verified the superiority of the proposed adaptive protocols compared to benchmark schemes from the literature, especially when the FSO links suffered from severe

atmospheric impairments. Furthermore, even for an average delay of only 20 time slots, the proposed delay-constrained BA protocol considerably outperformed the optimal non-BA protocol and achieved a performance close to that of the optimal delay-unconstrained BA protocol.

APPENDIX A

PROOF OF THEOREM 1

In this appendix, we derive the solution to the optimization problem in (7). To this end, we first specify the potential candidates for the optimal relay selection policy among all possible relay selection policies $(\alpha_{lm}, \beta_{lm})$. Subsequently, we derive the optimal RF time allocation policy ρ_i^* for each of the potential candidates for the optimal relay selection policy. Finally, the relay selection policy which yields the maximum end-to-end throughput among the candidate relay selection policies is chosen as the optimal relay selection policy $(\alpha_{lm}^*, \beta_{lm}^*)$.

A. Candidate Policies

The feasible sets \mathcal{A} and \mathcal{B} of the relay selection variables allow the selection of at most four different relays for RF/FSO reception and transmission. Therefore, there are in total M^4 possibilities for the optimal binary values of α_{lm} and β_{lm} in the feasible set $\mathcal{A} \times \mathcal{B}$. However, due to the constraints in (7), the optimal relay selection policy can select at most two different relays for RF/FSO reception and transmission in order to ensure that the data which is transmitted from the source to a certain relay can be actually forwarded to the destination. Thereby, there are $\frac{M(M-1)}{2}$ possibilities to select two relays out of M relays. Moreover, for a given selected relay pair, there are $2^4 = 16$ possibilities to assign the selected relays to RF/FSO reception and transmission, respectively. In the following, we show that only 6 among these 16 possibilities are candidates for the optimal relay selection policy. To this end, let m and n be the indices of the selected relays. Considering the feasible sets \mathcal{A} and \mathcal{B} , we investigate the following $2^2 = 4$ possibilities for the RF/FSO receiving relays: *i*) Relay m is selected for both RF/FSO reception, i.e., $\alpha_{1m} = \beta_{1m} = 1$. In this case, relay m is the only option for RF/FSO transmission, i.e., $\alpha_{2m} = \beta_{2m} = 1$ has to hold (hybrid mode). *ii*) Relay m is selected for RF reception and relay n is selected for FSO reception, i.e., $\alpha_{1n} = \beta_{1m} = 1$. Here, there are two options, namely, relays m and n are chosen either for RF and FSO transmission, respectively, i.e., $\alpha_{2n} = \beta_{2m} = 1$ (independent mode), or for FSO and RF transmission, respectively, i.e., $\alpha_{2m} = \beta_{2n} = 1$ (mixed mode). Cases *iii*) and *iv*) are identical to Cases *i*) and *ii*), respectively, after changing the roles of relays n and m . To summarize, among the M^4 possibilities for α_{lm} and β_{lm} in the feasible set $\mathcal{A} \times \mathcal{B}$, only $3M(M-1)$ possibilities have to be investigated for the optimal relay selection policy.

B. Optimal RF Time Allocation

In the following, the optimal RF time allocation policy ρ_l^* and the resulting throughput are derived for the aforementioned $3M(M-1)$ possibilities depending on their modes of transmission, namely the hybrid, independent, and mixed modes.

Case 1 (Hybrid Mode): Suppose relay \mathcal{R}_m is selected for both RF/FSO transmission/reception. Thereby, the optimal ρ_l is found such that the minimum of the capacities of the $\mathcal{S} - \mathcal{R}_m$ hybrid RF/FSO link and the $\mathcal{R}_m - \mathcal{D}$ hybrid RF/FSO link is maximized, i.e.,

$$\rho_1 = 1 - \rho_2 = \left[\frac{C_{2m}^{\text{fso}} + C_{2m}^{\text{rf}} - C_{1m}^{\text{fso}}}{C_{1m}^{\text{rf}} + C_{2m}^{\text{rf}}} \right]_0^1, \quad (24)$$

which leads to the overall throughput τ_m^{hyb} given in (9a). Moreover, the optimal relay for RF and FSO transmission is the one which leads to the maximum value of τ_m^{hyb} in (9a), i.e., the index of the optimal relay is given by $m^* = \underset{m}{\operatorname{argmax}} \tau_m^{\text{hyb}}$.

Case 2 (Independent Mode): Let relay \mathcal{R}_m be selected for both FSO reception and transmission and a different relay \mathcal{R}_n be selected for RF reception and transmission. The optimal ρ_l which makes the RF transmission rates of the $\mathcal{S} - \mathcal{R}_n$ and $\mathcal{R}_n - \mathcal{D}$ links equal is found as

$$\rho_1 = 1 - \rho_2 = \frac{C_{2n}^{\text{rf}}}{C_{1n}^{\text{rf}} + C_{2n}^{\text{rf}}}. \quad (25)$$

This leads to the overall throughput τ_{mn}^{ind} given in (9b). Moreover, in this case, we can independently select the relay which maximizes the throughput of FSO transmission, i.e., $m^* = \underset{m}{\operatorname{argmax}} \tau_m^{\text{fso}}$, and the relay which maximizes the throughput of RF transmission, i.e., $n^* = \underset{n}{\operatorname{argmax}} \tau_n^{\text{rf}}$.

Case 3 (Mixed Mode): Here, different relays \mathcal{R}_m and \mathcal{R}_n are selected for FSO reception and transmission, respectively. Moreover, for this case to be optimal, relays \mathcal{R}_m and \mathcal{R}_n have to be selected for RF transmission and RF reception, respectively. For this case, we can distinguish the following four subcases depending on which links are the bottleneck for data transmission.

Subcase 1: The bottleneck links for both relays \mathcal{R}_m and \mathcal{R}_n are the FSO links. Hence, the RF time sharing variables have to be chosen to support the FSO links, i.e., $\rho_1 \geq \frac{C_{2n}^{\text{fso}}}{C_{1n}^{\text{rf}}}$ and $\rho_2 \geq \frac{C_{1m}^{\text{fso}}}{C_{2m}^{\text{rf}}}$. Therefore, a necessary condition for this subcase to be optimal is that $\frac{C_{2n}^{\text{fso}}}{C_{1n}^{\text{rf}}} + \frac{C_{1m}^{\text{fso}}}{C_{2m}^{\text{rf}}} \leq 1$ holds. Without loss of generality and since $\rho_1 + \rho_2 = 1$ has to hold, we choose the following solution

$$\rho_1 = 1 - \rho_2 = \frac{C_{2n}^{\text{fso}}}{C_{1n}^{\text{rf}}}. \quad (26)$$

This subcase leads to throughput $\tau = C_{1m}^{\text{fso}} + C_{2n}^{\text{fso}}$.

Subcase 2: The bottleneck links for both relays \mathcal{R}_m and \mathcal{R}_n are the RF links. This leads to

throughput $\tau = \rho_1 C_{1n}^{\text{rf}} + \rho_2 C_{2m}^{\text{rf}}$. Hence, we obtain

$$\rho_1 = 1 - \rho_2 = \begin{cases} 1, & \text{if } C_{1n}^{\text{rf}} \geq C_{2m}^{\text{rf}} \\ 0, & \text{otherwise.} \end{cases} \quad (27)$$

However, the RF transmission time allocation policy in (27) implies that the RF link is selected to support either FSO transmission or reception, i.e., only one of the relays is active. Therefore, this subcase cannot be optimal since Case 1 always yields a higher throughput.

Subcase 3: The bottleneck links for relays \mathcal{R}_m and \mathcal{R}_n are the FSO and RF links, respectively. This leads to throughput $\tau = C_{1m}^{\text{fso}} + \rho_1 C_{1n}^{\text{rf}}$. Here, the throughput can be always improved by increasing ρ_1 and decreasing ρ_2 until the $\mathcal{S} - \mathcal{R}_m$ FSO link is no longer the bottleneck. This contradicts the earlier assumption of this subcase, i.e., Subcase 3 cannot occur for the optimal solution.

Subcase 4: The bottleneck links for relays \mathcal{R}_m and \mathcal{R}_n are the RF and FSO links, respectively. Similar to Subcase 3, Subcase 4 cannot occur for the optimal solution.

To conclude, among the four possible subcases for Case 3, only Subcase 1 can be the optimal solution for some fading realizations. Hence, without loss of generality, we define the throughput of Case 3, denoted by τ_{mn}^{mix} , in (9c) as the throughput of Subcase 1 if the necessary condition for this subcase, i.e., $\frac{C_{2n}^{\text{fso}}}{C_{1n}^{\text{rf}}} + \frac{C_{1m}^{\text{fso}}}{C_{2m}^{\text{rf}}} \leq 1$ holds, and zero otherwise. The indices of the optimal relays are given by $(m^*, n^*) = \underset{(m,n)}{\operatorname{argmax}} \tau_{mn}^{\text{mix}}$.

C. Optimal Policy

Now, the remaining question is in which mode the RF and FSO links should operate for a given channel realization. Since our goal is to maximize the throughput, we have to select the case which yields the maximum achievable throughput, i.e., the maximum value among $\tau_{m^*}^{\text{hyb}}$, $\tau_{m^*}^{\text{fso}} + \tau_{n^*}^{\text{rf}}$, and $\tau_{m^*n^*}^{\text{mix}}$. This leads to the relay selection policy given in Theorem 1 and completes the proof.

APPENDIX B

PROOF OF THEOREM 2

In this appendix, our aim is to solve the optimization problem in (14). The problem in (14) is non-convex because of the binary constraints on $\alpha_{lm}[b]$ and $\beta_{lm}[b]$ and the multiplication of two variables, $\beta_{lm}[b]\rho_l[b]$. To make the problem tractable, we relax the binary constraint $\alpha_{lm}[b] \in \{0, 1\}$ to $\alpha_{lm}[b] \in [0, 1]$ and define new variable $\gamma_{lm}[b] \triangleq \beta_{lm}[b]\rho_l[b]$. The feasible sets of the new variables of the relaxed problem are given by $\alpha_{lm}[b] \in \tilde{\mathcal{A}} = \{\alpha | \alpha_{lm}[b] \in [0, 1], \forall l, m, b \wedge \sum_{\forall m} \alpha_{lm}[b] = 1, \forall l, b\}$ and $\gamma_{lm}[b] \in \mathcal{G} = \{\gamma | \gamma_{lm}[b] \in [0, 1], \forall l, m, b \wedge \sum_{\forall l} \sum_{\forall m} \gamma_{lm}[b] = 1, \forall b\}$ where γ is a vector containing the $\gamma_{lm}[b], \forall l, m, b$. The relaxed problem is linear and can be solved globally using

the dual Lagrange method [31]. Moreover, we will show that the solution of the relaxed problem is binary, and hence, also solves the original problem in (14). In particular, the Lagrangian function corresponding to the relaxed version of the optimization problem in (14) is obtained as

$$\begin{aligned} \mathcal{L}(\bar{\tau}, \alpha, \gamma, \bar{\lambda}) = & \sum_{\forall m} \bar{\tau}_m + \sum_{\forall m} \lambda_{1m} \left(\frac{1}{B} \sum_{\forall b} [\alpha_{1m}[b] C_{1m}^{\text{fso}}[b] + \gamma_{1m}[b] C_{1m}^{\text{rf}}[b]] - \bar{\tau}_m \right) \\ & + \sum_{\forall m} \lambda_{2m} \left(\frac{1}{B} \sum_{\forall b} [\alpha_{2m}[b] C_{2m}^{\text{fso}}[b] + \gamma_{2m}[b] C_{2m}^{\text{rf}}[b]] - \bar{\tau}_m \right), \end{aligned} \quad (28)$$

where $\bar{\lambda}$ is a vector containing all Lagrange multipliers corresponding to the constraints in (14), i.e., $\lambda_{lm}, \forall m, l$. The dual function and the dual problem are given by

$$\mathcal{D}(\bar{\lambda}) = \underset{\bar{\tau} \geq \mathbf{0}, \alpha \in \bar{\mathcal{A}}, \gamma \in \mathcal{G}}{\text{maximize}} \quad \mathcal{L}(\bar{\tau}, \alpha, \gamma, \bar{\lambda}) \quad (29)$$

$$\text{and } \underset{\bar{\lambda} \geq \mathbf{0}}{\text{minimize}} \quad \mathcal{D}(\bar{\lambda}), \quad (30)$$

respectively. To solve (14) using the dual problem in (30), we first obtain primal variables $\bar{\tau}$, α , and γ for a given vector of dual variables $\bar{\lambda}$. Then, we find the dual variables $\bar{\lambda}$ from (30).

A. Optimal Primal Variables

The optimal primal variables are either boundary points of their feasible sets or stationary points which can be obtained by setting the derivatives of the Lagrangian function in (28) with respect to $\bar{\tau}$, α , and γ to zero. The derivatives of the Lagrangian function are obtained as

$$\frac{\partial \mathcal{L}}{\partial \alpha_{lm}[b]} = \frac{1}{B} \lambda_{lm} C_{lm}^{\text{fso}}[b] \triangleq \frac{1}{B} \Lambda_{lm}^{\text{fso}}[b], \quad (31a)$$

$$\frac{\partial \mathcal{L}}{\partial \gamma_{lm}[b]} = \frac{1}{B} \lambda_{lm} C_{lm}^{\text{rf}}[b] \triangleq \frac{1}{B} \Lambda_{lm}^{\text{rf}}[b], \quad (31b)$$

$$\frac{\partial \mathcal{L}}{\partial \bar{\tau}_m} = 1 - \lambda_{1m} - \lambda_{2m}. \quad (31c)$$

Since $\lambda_{lm} \geq 0$ holds due to dual feasibility condition [31], the derivative $\frac{\partial \mathcal{L}}{\partial \alpha_{lm}[b]}$ in (31a) is always positive. On the other hand, $\sum_{\forall m} \alpha_{lm}[b] = 1$ has to hold for $l = 1, 2$. Therefore, for FSO reception, the optimal protocol selects the $\mathcal{S} - \mathcal{R}_m$ FSO link with the maximum selection metric, $\Lambda_{1m}^{\text{fso}}[b]$, in each time slot. We note that since the pdfs of the fading distributions are continuous, the probability that two selection metrics are equal is zero. Analogously, for FSO transmission, the $\mathcal{R}_m - \mathcal{D}$ FSO link with the maximum $\Lambda_{2m}^{\text{fso}}[b]$ will be selected. Similarly, the derivative $\frac{\partial \mathcal{L}}{\partial \gamma_{lm}[b]}$ in (31b) is positive and $\sum_{\forall l} \sum_{\forall m} \gamma_{lm}[b] = 1$ has to hold, which leads to $\gamma_{lm}[b] = 1$ for the largest $\Lambda_{lm}^{\text{rf}}[b]$, $\forall l, m$ and zero for the rest. Since $\gamma_{lm}[b] = \rho_l[b] \beta_{lm}[b]$, $\gamma_{lm}[b] = 1$ leads to a unique solution for $\rho_l[b] = 1$

and $\beta_{lm}[b] = 1$. Moreover, since $\rho_l[b] = 1$ holds, we obtain that $\rho_{l'}[b] = 0$, $l' \neq l$. Therefore, the throughput does not change irrespective for which relay index m $\beta_{l'm}[b] = 1$ holds. Note that unique binary values are obtained for the variables of the original problem based on the optimal values of the relaxed variables. Hence, the employed relaxation also yields the optimal solution for the original problem in (14). These results are concisely stated in (15a), (15b), and (15c) in Theorem 2.

If $\frac{\partial \mathcal{L}}{\partial \bar{\tau}_m} > 0$ holds, the optimal value of $\bar{\tau}_m$ is at the boundary of its feasible set, i.e., $\bar{\tau}_m \rightarrow \infty$, which cannot be the optimal solution. Similarly, if $\frac{\partial \mathcal{L}}{\partial \bar{\tau}_m} < 0$ holds, the optimal value of $\bar{\tau}_m$ is at the boundary of its feasible set, i.e., $\bar{\tau}_m \rightarrow 0$, which results in $\lambda_{1m} + \lambda_{2m} > 1$. In addition, recall that $\lambda_{lm} \geq 0$ has to hold due to dual feasibility condition [31]. Therefore, either λ_{1m} or λ_{2m} is positive. Suppose $\lambda_{1m} > 0$ ($\lambda_{2m} > 0$) holds, then the value of RV $\Lambda_{1m}^{\text{fso}}[b]$ ($\Lambda_{2m}^{\text{fso}}[b]$) is greater than the value of $\Lambda_{1m'}^{\text{fso}}[b]$ ($\Lambda_{2m'}^{\text{fso}}[b]$), $\forall m' \neq m$ with a non-zero probability. Consequently, the optimal protocol will select the $\mathcal{S} - \mathcal{R}_m$ ($\mathcal{R}_m - \mathcal{D}$) FSO link while the end-to-end throughput achieved by \mathcal{R}_m is zero, i.e., $\bar{\tau}_m \rightarrow 0$. This is a contradiction. Therefore, the derivative $\frac{\partial \mathcal{L}}{\partial \bar{\tau}_m}$ in (31c) has to be zero which leads to $\lambda_{1m} + \lambda_{2m} = 1$.

B. Optimal Dual Variables

Let us first introduce a new variable $\lambda_m \triangleq \lambda_{1m} = 1 - \lambda_{2m}$ and vector $\boldsymbol{\lambda}$ which contains all variables $\lambda_m, \forall m$. Hence, by substituting the optimal value of $\boldsymbol{\alpha}$, $\boldsymbol{\gamma}$, and $\bar{\boldsymbol{\tau}}$ into the Lagrangian function in (28), the dual function in (29) can be rewritten as

$$\begin{aligned} \mathcal{D}(\boldsymbol{\lambda}) &= \sum_{\forall m} \bar{\tau}_m + \sum_{\forall m} \lambda_m (\bar{C}_{1m}^{\text{fso}} + \bar{C}_{1m}^{\text{rf}} - \bar{\tau}_m) + \sum_{\forall m} (1 - \lambda_m) (\bar{C}_{2m}^{\text{fso}} + \bar{C}_{2m}^{\text{rf}} - \bar{\tau}_m) \\ &= \sum_{\forall m} \left(\lambda_m (\bar{C}_{1m}^{\text{fso}} + \bar{C}_{1m}^{\text{rf}}) + (1 - \lambda_m) (\bar{C}_{2m}^{\text{fso}} + \bar{C}_{2m}^{\text{rf}}) \right), \end{aligned} \quad (32)$$

where $\bar{C}_{lm}^{\text{fso}} = \frac{1}{B} \sum_{\forall b} \alpha_{lm}[b] C_{lm}^{\text{fso}}[b]$ and $\bar{C}_{lm}^{\text{rf}} = \frac{1}{B} \sum_{\forall b} \gamma_{lm}[b] C_{lm}^{\text{rf}}[b]$, $l = 1, 2$.

The optimal value of $\boldsymbol{\lambda}$ can be obtained by solving the dual problem in (30). In order to solve the dual problem, we use the well-known sub-gradient method [31]. To minimize $\mathcal{D}(\boldsymbol{\lambda})$, the sub-gradient method updates all component of $\boldsymbol{\lambda}$ using the following update equation in iteration k

$$\lambda_m[k+1] = \left[\lambda_m[k] - \epsilon_m[k] \frac{\partial \mathcal{D}(\boldsymbol{\lambda})}{\partial \lambda_m} \right]_0^1, \quad (33)$$

where $\epsilon_m[k]$ is a small step size in the k -th iteration. Moreover, $[\cdot]_0^1$ is used since $0 \leq \lambda_m \leq 1$ has to hold. Substituting the derivative of the dual function into (33) leads to (16) in Theorem 2. The results in this appendix are concisely stated in Theorem 2 which completes the proof.

REFERENCES

- [1] F. Demers, H. Yanikomeroglu, and M. St-Hilaire, "A Survey of Opportunities for Free Space Optics in Next Generation Cellular Networks," in *Proc CNSR*, May 2011, pp. 210–216.
- [2] M. Corson, R. Laroia, J. Li, V. Park, T. Richardson, and G. Tsirtsis, "Toward Proximity-Aware Internetworking," *IEEE Wireless Commun.*, vol. 17, no. 6, pp. 26–33, Dec. 2010.
- [3] Analysys Mason Report S. Hilton, "Machine-to-Machine Device Connections: Worldwide Forecast 2010-2020," *Analysys Mason Report*, 2010.
- [4] M. Khalighi and M. Uysal, "Survey on Free Space Optical Communication: A Communication Theory Perspective," *IEEE Commun. Surveys Tutorials*, vol. 16, no. 4, pp. 2231–2258, 2014.
- [5] H. Kaushal and G. Kaddoum, "Free Space Optical Communication: Challenges and Mitigation Techniques," *Online version available on arXiv*, Jun. 2015. [Online]. Available: <http://arxiv.org/abs/1506.04836>
- [6] C. Abou-Rjeily, "All-Active and Selective FSO Relaying: Do We Need Inter-Relay Cooperation?" *J. Lightw. Technol.*, vol. 32, no. 10, pp. 1899–1906, May 2014.
- [7] M. Kashani, M. Safari, and M. Uysal, "Optimal Relay Placement and Diversity Analysis of Relay-Assisted Free-Space Optical Communication Systems," *IEEE/OSA J. Opt. Commun. Net.*, vol. 5, no. 1, pp. 37–47, Jan. 2013.
- [8] C. Abou-Rjeily, "Performance Analysis of FSO Communications with Diversity Methods: Add More Relays or More Apertures?" *IEEE J. Sel. Areas Commun.*, vol. 33, no. 9, pp. 1890–1902, Sep. 2015.
- [9] N. Chatzidiamantis, D. Michalopoulos, E. Kriezis, G. Karagiannidis, and R. Schober, "Relay Selection Protocols for Relay-Assisted Free-Space Optical Systems," *IEEE/OSA J. Opt. Commun. Net.*, vol. 5, no. 1, pp. 92–103, Jan. 2013.
- [10] M. Petkovic, A. Cvetkovic, G. Djordjevic, and G. Karagiannidis, "Partial Relay Selection with Outdated Channel State Estimation in Mixed RF/FSO Systems," *J. Lightw. Technol.*, vol. 33, no. 13, pp. 2860–2867, Jul. 2015.
- [11] M. Usman, H. Yang, and M.-S. Alouini, "Practical Switching-Based Hybrid FSO/RF Transmission and its Performance Analysis," *IEEE Photonics J.*, vol. 6, no. 5, pp. 1–13, Oct. 2014.
- [12] B. He and R. Schober, "Bit-Interleaved Coded Modulation for Hybrid RF/FSO Systems," *IEEE Trans. Commun.*, vol. 57, no. 12, pp. 3753–3763, Dec. 2009.
- [13] V. Jamali, D. S. Michalopoulos, M. Uysal, and R. Schober, "Link Allocation for Multiuser Systems With Hybrid RF/FSO Backhaul: Delay-Limited and Delay-Tolerant Designs," *IEEE Trans. Wireless Commun.*, vol. 15, no. 5, pp. 3281–3295, May 2016.
- [14] M. Najafi, V. Jamali, and R. Schober, "Adaptive Relay Selection Protocol for the Parallel Hybrid RF/FSO Relay Channel," in *Proc. IEEE Int. Conf. Commun. (ICC)*, May 2016, pp. 1–7.
- [15] N. Wang, E. Hossain, and V. K. Bhargava, "Backhauling 5G Small Cells: A Radio Resource Management Perspective," *IEEE Wireless Commun.*, vol. 22, no. 5, pp. 41–49, Oct. 2015.
- [16] J.-Y. Wang, J.-B. Wang, M. Chen, and X. Song, "Performance Analysis for Free-Space Optical Communications using Parallel All-Optical Relays over Composite Channels," *IET Commun.*, vol. 8, no. 9, pp. 1437–1446, Jun. 2014.
- [17] M. Duarte, C. Dick, and A. Sabharwal, "Experiment-Driven Characterization of Full-Duplex Wireless Systems," *IEEE Trans. Wireless Commun.*, vol. 11, no. 12, pp. 4296–4307, Dec. 2012.
- [18] N. Nomikos, T. Charalambous, I. Krikidis, D. Skoutas, D. Vouyioukas, M. Johansson, and C. Skianis, "A Survey on Buffer-Aided Relay Selection," *IEEE Commun. Surveys Tutorials*, vol. 18, no. 2, pp. 1073–1097, 2016.
- [19] A. Ikhlef, D. Michalopoulos, and R. Schober, "Max-Max Relay Selection for Relays with Buffers," *IEEE Trans. Wireless Commun.*, vol. 11, no. 3, pp. 1124–1135, Mar. 2012.
- [20] I. Krikidis, T. Charalambous, and J. Thompson, "Buffer-Aided Relay Selection for Cooperative Diversity Systems without Delay Constraints," *IEEE Trans. Wireless Commun.*, vol. 11, no. 5, pp. 1957–1967, May 2012.
- [21] W. Zhang, S. Hranilovic, and C. Shi, "Soft-Switching Hybrid FSO/RF Links Using Short-Length Raptor Codes: Design and Implementation," *IEEE J. Sel. Areas Commun.*, vol. 27, no. 9, pp. 1698–1708, Dec. 2009.

- [22] P. McIllree, "Calculation of Channel Capacity for M-ary Digital Modulation Signal Sets," in *Proc. IEEE Singapore Int. Conf. Inf. Engineering, Commun., Net.*, vol. 2, Sep. 1993, pp. 639–643 vol.2.
- [23] T. M. Cover and J. A. Thomas, *Elements of Information Theory*. Wiley, John and Sons, Incorporated, 1991.
- [24] N. Vaiopoulos, H. Sandalidis, and D. Varoutas, "WiMAX on FSO: Outage Probability Analysis," *IEEE Trans. Commun.*, vol. 60, no. 10, pp. 2789–2795, Oct. 2012.
- [25] N. Letzepis, K. D. Nguyen, A. G. Fabregas, and W. G. Cowley, "Outage Analysis of the Hybrid Free-Space Optical and Radio-Frequency Channel," *IEEE J. Sel. Areas Commun.*, vol. 27, no. 9, pp. 1709–1719, Dec. 2009.
- [26] M. J. Neely, "Stochastic Network Optimization with Application to Communication and Queueing Systems," *Synthesis Lectures on Commun. Net.*, vol. 3, no. 1, pp. 1–211, 2010.
- [27] V. Jamali, N. Zlatanov, A. Ikhlef, and R. Schober, "Achievable Rate Region of Bidirectional Buffer-Aided Relay Channel with Block Fading," *IEEE Trans. Inf. Theory*, vol. 60, no. 11, pp. 7090–7111, Nov. 2014.
- [28] J. D. C. Little, "A Proof for the Queuing Formula: $L = \lambda W$," *Operations Research*, vol. 9, no. 3, pp. 383–387, 1961.
- [29] N. Zlatanov, V. Jamali, and R. Schober, "Achievable Rates for the Fading Half-Duplex Single Relay Selection Network Using Buffer-Aided Relaying," *IEEE Trans. Wireless Commun.*, vol. 14, no. 8, pp. 4494–4507, Aug. 2015.
- [30] A. Bletsas, A. Khisti, D. Reed, and A. Lippman, "A Simple Cooperative Diversity Method Based on Network Path Selection," *IEEE J. Sel. Areas Commun.*, vol. 24, no. 3, pp. 659–672, Mar. 2006.
- [31] S. Boyd and L. Vandenberghe, *Convex Optimization*. Cambridge, U.K.: Cambridge Univ. Press, 2004.